

Aus der Franz-Volhard-Klinik  
am Max-Delbrück-Centrum für molekulare Medizin  
der Medizinischen Fakultät Charité  
der Humboldt-Universität zu Berlin

## **DISSERTATION**

**Genetic analysis in hypertrophic cardiomyopathy:  
missense mutations in the ventricular myosin regulatory light chain gene**

zur Erlangung des akademischen Grades  
Doctor medicinae (Dr. med.)

vorgelegt der Medizinischen Fakultät Charité  
der Humboldt-Universität zu Berlin

von

Zhyldyz Kabaeva

aus Djany-Alysh (Kyrgyzstan)

Dekan / Dean: Prof. Dr. Joachim W. Dudenhausen

Gutachter / Reviewer:

1. Prof. Dr. med. Karl Josef Osterziel
2. Prof. Dr. med. Andreas Mügge
3. Prof. Dr. med. Hans-Peter Vosberg

Datum der Promotion / Date of the defence 11.11.2002

## Abstract

Hypertrophic cardiomyopathy (HCM) is a heart disorder characterized by unexplained ventricular myocardial hypertrophy and a high risk of sudden cardiac death. The disease is inherited as an autosomal-dominant trait. Nine disease-causing genes have been described all encoding for sarcomeric proteins. Mutations in the ventricular myosin essential (ELC) and regulatory (RLC) light chain genes are responsible approximately for 1% and 1 - 7% of all HCM cases, respectively. Limited data are available on the disease course and prognosis in HCM caused by mutations in these genes. Therefore, the present study was aimed to analyse the ELC and RLC genes for disease-causing mutations in a group of clinically well-characterized HCM patients. Further purpose was to assess whether the detected mutations are associated with malignant or benign phenotype in the respective families.

**Methods:** 71 unrelated patients with HCM and 14 family members were evaluated using physical examination, ECG and echocardiography. DNA was extracted from blood lymphocytes. Screening of the 6 exons of the ELC gene and the 7 exons of the RLC gene was done by using PCR and single strand conformation polymorphism analysis (SSCP). Samples with aberrant band patterns were directly sequenced.

**Results:** Systematic analysis revealed no mutation in the ELC gene but two disease-associated mutations leading to an amino acid exchange in the RLC gene. The first mutation was found in exon 2 of the RLC gene: a G>A nucleotide substitution at position c.64 caused a replacement of glutamic acid by lysine at codon 22. The second mutation was in exon 4 of the RLC gene: a G>A substitution at nucleotide c.173 led to a change of arginine to glutamine at codon 58. Both mutations affected highly conserved amino acids and were located in the amino terminal half of the RLC close to the putative phosphorylation and calcium-binding sites. They also changed overall electrical charge of this protein region. The Glu22Lys mutation was identified in seven individuals of family K and was associated with moderate septal hypertrophy, a late onset of clinical manifestation, benign disease course, and good prognosis. The mutation Arg58Gln showed also moderate septal hypertrophy, but, in contrast, it was associated with an early onset of clinical manifestation and premature sudden cardiac death in family B.

Additionally, a number of sequence differences from reference genomic sequences, one silent mutation, and two single nucleotide polymorphisms (SNPs) were identified while screening the ELC and RLC genes. Detected SNPs did not cause an amino acid exchange and did not affect splicing process proceeding from their localisation.

**Conclusions:** Two missense mutations were identified in the ventricular myosin regulatory light chain gene and associated with either benign or malignant HCM phenotypes. These findings show that genotyping could give valuable information for risk stratification, genetic counselling, and treatment strategies in hypertrophic cardiomyopathy.

**Keywords:** Genetics, Cardiomyopathy, Hypertrophy, Sudden cardiac death

## Zusammenfassung

Die Hypertrophe Kardiomyopathie (*Hypertrophic Cardiomyopathy*, HCM) ist eine Erkrankung des Herzens, die durch eine Hypertrophie des Myokards und einem erhöhten Risiko für den plötzlichen Herztod charakterisiert ist. Die Erkrankung wird autosomal-dominant vererbt. Neun HCM-assoziierte Genen wurden bisher beschrieben, die alle für Sarkomer-Proteine kodierend. Mutationen in den Genen für die essentielle (ELC) und regulatorische (RLC) leichte Myosin-Kette sind für ca. 1% bzw. 1-7% aller HCM-Fälle verantwortlich. Bisher gibt es nur wenige Informationen zum Krankheitsverlauf und zur Prognose bei HCM-Formen, die durch Mutationen in diesen Genen verursacht werden. Ziel dieser Studie war daher, das ELC- bzw. RLC-Gen in einem Kollektiv klinisch gut charakterisierter HCM-Patienten hinsichtlich möglicher krankheitsverursachender Mutationen zu analysieren. Darüber hinaus sollte untersucht werden, ob die hier identifizierten Mutationen mit einem malignen bzw. benignen Phänotyp assoziiert sind.

**Methoden:** 71 unverwandete Patienten mit primärer HCM wurden mittels körperlicher Untersuchung, EKG und Echokardiographie evaluiert. Die aus Blutlymphozyten extrahierte DNA wurde mittels exonspezifischer PCR-Amplifikation und Single-strand-conformation-polymorphism (SSCP) Analyse auf Mutationen in den 6 Exons des ELC- und 7 Exons des RLC-Gens untersucht. Proben mit auffälligen Bandenmustern wurden direkt sequenziert.

**Ergebnisse:** Die systematische Analyse ergab zwei krankheitsassoziierte Mutationen im RLC-Gen, die zu einem Aminosäureaustausch führen. Im ELC-Gen wurden keine Mutationen gefunden. Die erste Mutation im RLC-Gen ist ein G zu A-Basenaustausch an Position c.64 im Exon 2, der zu einem Austausch von Glutamat durch Lysin im Codon 22 führt. Die zweite Variante verursacht eine Argininsubstitution durch Glutamin im Codon 58 aufgrund eines Basenpaaraustausches an Position c.173 im Exon 4 (G zu A). Beide Mutationen betreffen hoch-konservierte Aminosäuren in der amino-terminalen Domäne des RLC in der Nähe von möglichen Phosphorylierungs- bzw. Kalzium-Bindungsstellen. Zusätzlich wird die elektrische Ladung dieser Proteinregion durch den Aminosäureaustausch verändert. Die Glu22Lys-Mutationen konnte in sieben Individuen der Familie K identifiziert werden und ist mit einer geringen septalen Hypertrophie, einer späten klinischen Manifestation sowie einem benignen

Verlauf und einer guten Prognose assoziiert. Die Arg58Gln-Mutation ist ebenfalls mit einer moderaten Septumhypertrophie aber mit einem frühen Krankheitsbeginn und einem vorzeitigen Auftreten eines plötzlichen Herztodes in der Familie B assoziiert.

Zusätzlich wurden mehrere Abweichungen von der Referenz-Sequenz, eine stumme Mutation sowie zwei "Single Nucleotide Polymorphisms" (SNPs) während des Screenings in beiden Genen identifiziert. Die SNPs verursachen keinen Aminosäureaustausch und beeinflussen nicht den Spleißvorgang, soweit dies durch ihre Lokalisation vorhersagbar ist.

**Schlussfolgerung:** Zwei missense Mutationen konnten in der regulatorischen leichten Myosinkette identifiziert und sowohl mit einem benignen als auch einem malignen HCM-Phänotyp assoziiert werden. Diese Ergebnisse zeigen, dass die Genotypisierung wertvolle Informationen für die Risikostratifizierung, die genetische Beratung sowie für Therapiestrategien in der Hypertrophe Kardiomyopathie liefern kann.

**Schlagwörter:** Genetik, Kardiomyopathie, Hypertrophie, plötzlicher Herztod

*with love and gratitude to my dear parents*

## Table of contents

<b>Abstract.....</b>	<b>iii</b>
<b>Zusammenfassung.....</b>	<b>v</b>
<b>1 Introduction .....</b>	<b>1</b>
1.1 Molecular genetics and pathogenesis of HCM .....	2
1.2 The ventricular myosin regulatory and essential light chains .....	8
1.3 Clinical features and diagnosis of HCM.....	9
1.4 Genotype-phenotype correlation studies.....	12
1.5 Aims of the present study .....	14
<b>2 Materials and methods .....</b>	<b>15</b>
2.1 Clinical evaluation .....	15
2.2 Genetic analysis .....	16
2.2.1 Approach overview.....	16
2.2.2 Preparation of genomic DNA.....	17
2.2.3 Amplification of coding exons of <i>MYL2</i> and <i>MYL3</i> .....	18
2.2.4 Single strand conformation polymorphism analysis .....	21
2.2.5 Automated DNA sequencing .....	24
2.2.6 Restriction fragment length polymorphism analysis .....	26
2.2.7 Agarose gel electrophoresis.....	27
2.3 Devices and Chemicals.....	28
2.3.1 Devices .....	28



2.3.2	Chemicals .....	29
<b>3</b>	<b>Results .....</b>	<b>31</b>
3.1	Patient characteristics .....	31
3.2	Genetic variants in human <i>MYL2</i> and <i>MYL3</i> .....	33
3.2.1	Identification of the Glu22Lys mutation in family K.....	35
3.2.2	Identification of the Arg58Gln mutation in family B.....	39
3.2.3	Localization of the mutations in highly conserved RLC regions .....	41
3.2.4	Clinical features of family K with the Glu22Lys mutation.....	43
3.2.5	Clinical features of family B with the Arg58Gln mutation.....	45
3.2.6	The c.420C>T (Phe140Phe) silent mutation in <i>MYL3</i> .....	46
3.2.7	Single nucleotide polymorphisms in <i>MYL2</i> .....	47
3.2.8	Genomic sequence differences.....	51
<b>4</b>	<b>Discussion .....</b>	<b>54</b>
4.1	Patient cohort and screening approach.....	54
4.2	The Glu22Lys and Arg58Gln mutations in <i>MYL2</i> .....	56
4.3	Genotype-phenotype correlations .....	58
4.4	Possible functional implications of the Glu22Lys and Arg58Gln mutations ....	61
<b>5</b>	<b>References .....</b>	<b>63</b>
	<b>List of abbreviations .....</b>	<b>70</b>
	<b>Appendix .....</b>	<b>I</b>
A.	Acknowledgements .....	I
B.	Curriculum Vitae.....	II
C.	Statement / Erklärung an Eides Statt .....	IV

## 1 Introduction

Hypertrophic Cardiomyopathy (HCM) is a heart disorder characterized by unexplained ventricular myocardial hypertrophy and a high risk of sudden cardiac death.<sup>1</sup> Myocardial hypertrophy is predominantly confined to the left ventricle (LV) and generally easily detectable by conventional echocardiography. The main diagnostic criterion for HCM is an increased LV wall thickness (normal  $\leq 12\text{mm}$ ) in the absence of other possible causes of myocardial hypertrophy as arterial hypertension, valvular disease, and others. HCM is also diagnosed pathologically by the presence of myocyte disarray and interstitial fibrosis along with myocyte hypertrophy.<sup>2</sup> The disease is caused by mutations in genes encoding for sarcomeric proteins. It can either be transmitted as an autosomal-dominant trait from an ill parent to a child or develop due to a *de novo* mutation.<sup>3</sup>

HCM is a relatively common genetically transmitted cardiovascular disease with a prevalence in the general population of about 0.2% (or 1 in 500).<sup>3,4</sup> The annual mortality rate for all HCM related deaths (sudden cardiac death, heart failure, and stroke) has been estimated as 1.4%, where the rate for sudden death is as high as 0.7%.<sup>5</sup> Young HCM patients are more prone to sudden cardiac death, however, elder patients are also in substantial risk of dying unexpectedly.<sup>5</sup>

## 1.1 Molecular genetics and pathogenesis of HCM

Since the first detailed description of HCM in 1958 by Teare,<sup>6</sup> research has been mainly directed on elucidating causes and pathogenesis of this disorder that could provide clues in earlier diagnosis, treatment, and prevention of the disease. Major advances have been made in understanding the etiologic factors of this disease. To date, mutations in nine genes all encoding for the cardiac sarcomeric proteins have been shown to cause HCM, however, mechanisms by which they lead to the disease are still not completely understood.

The first described gene was the one encoding for cardiac  $\beta$ -myosin heavy chain, the major contractile protein of the cardiac sarcomere.<sup>7</sup> Identification of mutations in two more sarcomeric components,  $\alpha$ -tropomyosin and cardiac troponin T,<sup>8</sup> in HCM patients led to the postulation that HCM results from defects in the sarcomeric proteins. HCM was subsequently referred to as a “disease of the sarcomere”.<sup>8</sup> Later, this postulation was supported by identification of mutations in the next six genes also encoding for the proteins of the cardiac sarcomere, namely, cardiac myosin binding protein-C,<sup>9</sup> ventricular myosin essential and regulatory light chains,<sup>10</sup> cardiac troponin I,<sup>11</sup> cardiac  $\alpha$ -actin,<sup>12</sup> and titin.<sup>13</sup>

The genes encoding for the sarcomeric proteins involved in HCM are located on different chromosomes and listed in table 1.1. As shown, the contribution of single gene mutations to HCM varies from less than 5% to 30%.<sup>3,14</sup> The most common causes are mutations in the  $\beta$ -myosin heavy chain, myosin binding protein-C, and cardiac troponin T genes accounting for approximately 70% of all HCM cases (table 1.1). Mutations in other genes are much less common. In total, more than 130 causal mutations have been identified, most of them in the  $\beta$ -myosin heavy chain gene. So far, only few mutations have been found in the titin, cardiac  $\alpha$ -actin, and ventricular myosin essential light chain genes.

**Table 1.1.** Sarcomeric proteins and genes responsible for HCM

Sarcomeric protein	Gene	Locus	Frequency	Number of mutations
$\beta$ -Myosin heavy chain	<i>MYH7</i>	14q12	~ 30%	70
Myosin binding protein-C	<i>MYBPC3</i>	11p11.2	~ 20%	29
Cardiac troponin T	<i>TNNT2</i>	1q32	~ 20%	14
$\alpha$ -Tropomyosin	<i>TPM1</i>	15q22.1	~ 5%	4
Cardiac troponin I	<i>TNNI3</i>	19p13.2	~ 5%	8
Cardiac $\alpha$ -actin	<i>ACTC</i>	15q14	< 5%	2
Titin	<i>TTN</i>	2q24.1	< 5%	1
Myosin light chain, regulatory (RLC)	<i>MYL2</i>	12q23-q24.3	1 - 7%*	8
Myosin light chain, essential (ELC)	<i>MYL3</i>	3p21.3-p21.2	~ 1%*	3

Note: adapted from ref. 3. \*From ref. 10, 15, and 16.

Genetically engineered animal models have been used efficiently to confirm the causality of sarcomeric protein mutations in HCM. Phenotypes similar to those found in human HCM were induced in transgenic mice expressing a sarcomeric protein carrying a certain human mutation, and in "knockout" mice, in which a particular sarcomeric protein gene was ablated by gene targeting.<sup>17</sup> The cardiac expression of the common  $\beta$ -myosin heavy chain mutation (Arg403Gln) in transgenic rabbits also induced hypertrophy, myocyte and myofibrillar disarray, interstitial fibrosis, and premature death, phenotypes observed in HCM patients carrying this mutation.<sup>18</sup> Development of animal models, in which disease progression can be studied closely over the lifespan of an animal, has also shed significant light into the pathogenesis of HCM.

The sarcomere is the contractile unit of striated muscle. As shown in figure 1.1, cardiac myocytes contain numerous myofibrils. Each myofibril is in turn composed of repeating sarcomere units separated by Z discs. Each sarcomere is a highly ordered complex array of numerous proteins, the precise organisation and alignment of which are essential for proper muscle function.<sup>19</sup> The overall organisation of the sarcomere is similar in all striated muscles, although the proteins constituting it have a number of isoforms, which are differentially expressed depending on the muscle type.

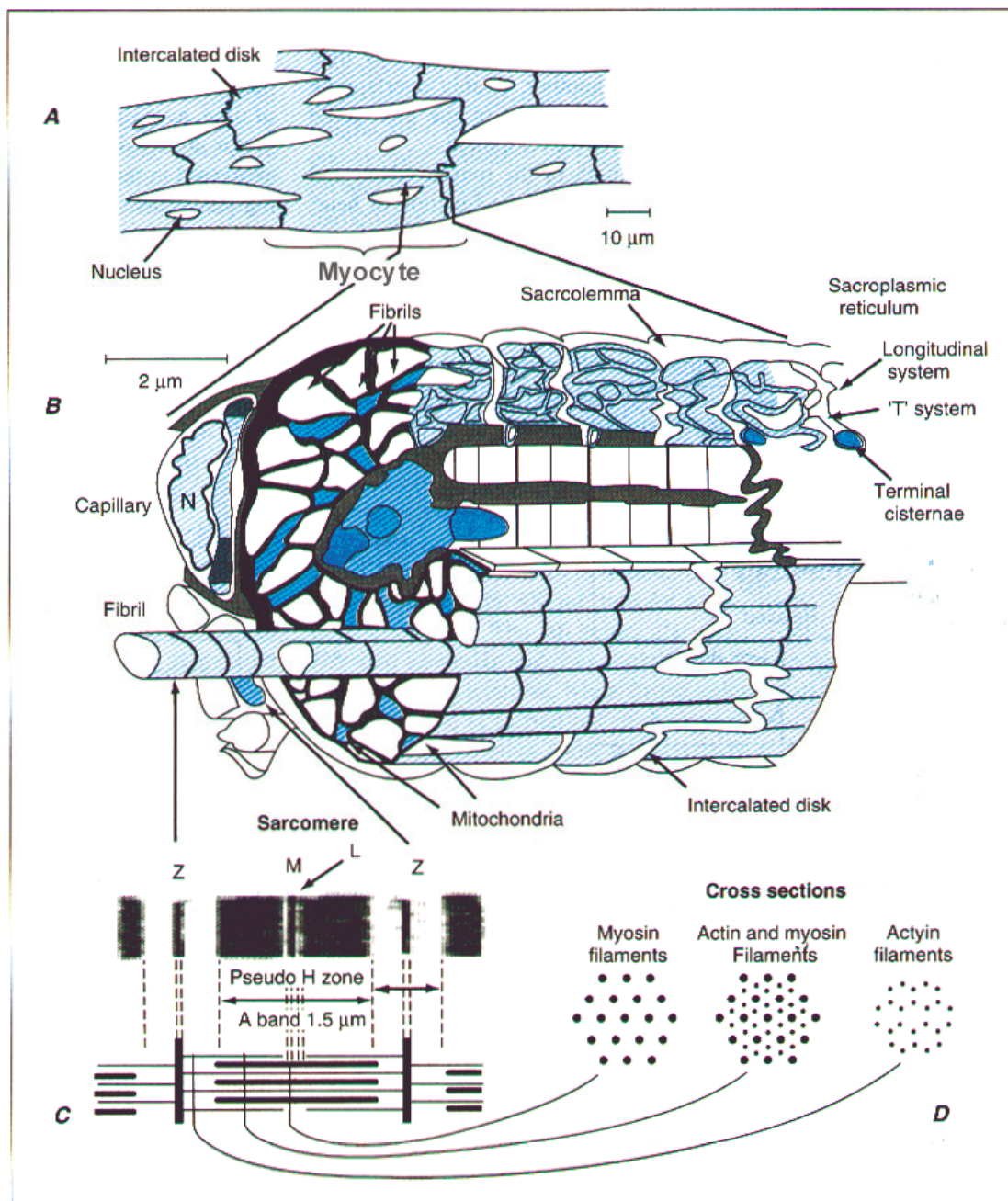


**Figure 1.1. Microscopic structure of heart muscle.** **A)** Myocardium as seen under the light microscope. Myocytes contain a centrally located nucleus and are connected across intercalated disks. **B)** Myocardial cell reconstituted from electron micrographs. Each myocyte is composed of multiple parallel fibrils. Each fibril is composed of serially connected sarcomeres (N, nucleus). **C)** Sarcomere from a myofibril, with diagrammatic representation of myofilaments. Thick filaments (1.5 µm long, composed of myosin) from the A band, and thin filaments (1 µm long, composed primarily of actin) extend from the Z line through the I band into the A band. The overlapping of thick and thin filaments is seen only in the A band. **D)** Cross sections of the sarcomere indicate the specific lattice arrangements of the myofilaments. In the center of the sarcomere only the thick, or myosin, filaments arranged in a hexagonal array are seen. In the distal portions of the A band, both thick and thin, or actin, filaments are found, with each thick filament surrounded by six thin filaments. In the I band only thin filaments are present. From ref. 20.

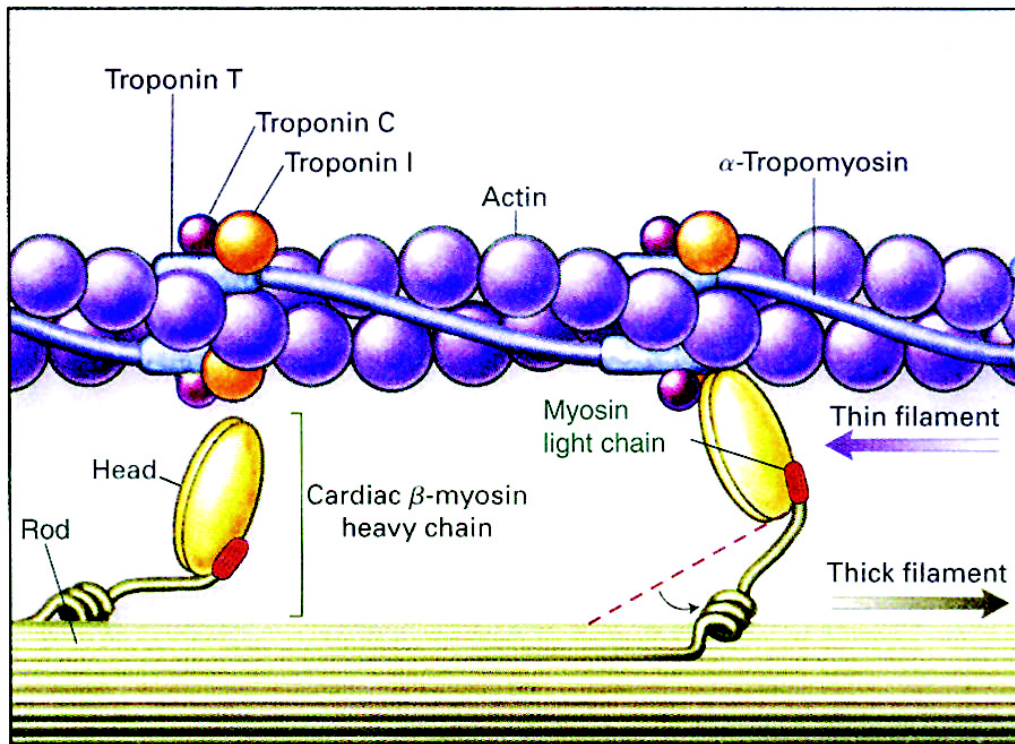


**Figure 1.2. Schematic diagram of sarcomere organisation and contraction process.** The thin filament is made up of actin, the troponin complex (T,C and I) and  $\alpha$ -tropomyosin. The thick filament is composed of myosin heavy and light chains. The sarcomere produces muscle contraction by sliding of myofilaments: the myosin heads interact with actin and pull it towards the center of the sarcomere resulting in shortening of the sarcomere. From ref. 2.

The sarcomere consists of overlapping arrays of thick and thin filaments, which shorten the length of the sarcomere during contraction by sliding past each other (figure 1.2). The thin filaments are attached to the Z discs. The thick filaments extend from the centre of the sarcomere in either direction towards the Z lines and are supported by binding to the protein-C and titin molecules. The major components of the thin filaments are cardiac  $\alpha$ -actin,  $\alpha$ -tropomyosin, and the troponin complex consisting of three subunits: troponin C, troponin I and troponin T. The thick filaments are composed of several hundreds of myosin molecules assembled together.

Myosin is called "molecular motor" of the sarcomere due to its ability to hydrolyse adenosine triphosphate (ATP) and thereby to transfer chemical energy into contraction force and motion.<sup>21</sup> Each myosin molecule is made up of two myosin heavy chains and two pairs of light chains (figure 1.3 A).

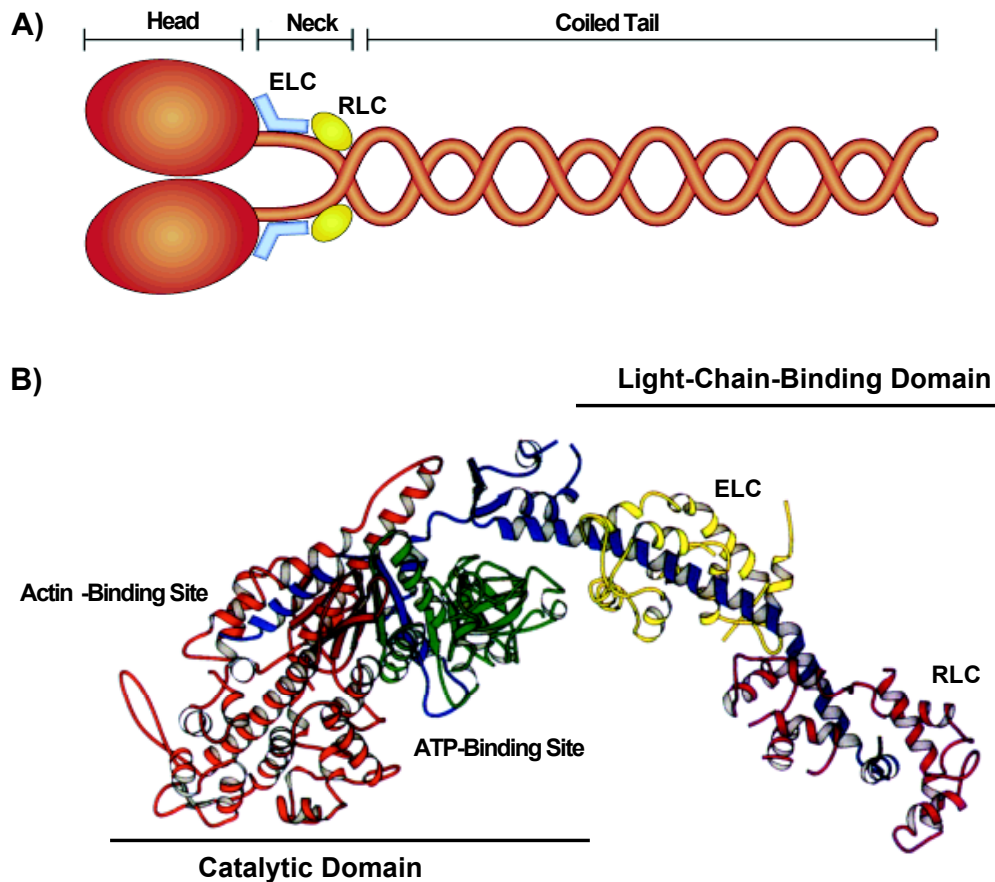


**Figure 1.3. A) Schematic representation of a myosin molecule constituting the thick filaments of the sarcomere.** The myosin molecule is a hexamer consisting of two heavy chains (orange), two essential light chains (blue) and two regulatory light chains (yellow). The myosin heavy chains are dimerized through their coiled-coil tails. Adapted from ref. 22.

**B) Three-dimensional (crystal) structure of a chicken skeletal myosin head.** The catalytic and light-chain-binding domains are indicated. The heavy chain is shown in red, green and blue. The essential (yellow) and regulatory (purple) light chains wrap around the heavy chain  $\alpha$ -helix (blue). Adapted from ref. 10 and 30.

The myosin heavy chain is a highly asymmetric molecule with a predominantly globular head and a rod like tail. The latter is formed by a coiled-coil structure of two  $\alpha$ -helices and accounts for the formation of the thick filament backbone. The globular head contains a light-chain-binding domain and a catalytic domain with actin- and ATP-binding sites as shown in figure 1.3 B depicting the three-dimensional structure of a chicken skeletal myosin head.<sup>21</sup>

The regulatory and essential light-chain-binding domain of myosin is also referred to as the neck region, because it connects the head with the myosin tail. As shown in figure 1.3 B, the essential light chain wraps around the amino terminal half of the myosin neck, whereas the regulatory light chain lies closer to the head-rod junction. Myosin light chains have several isoforms with some of them encoded by different genes. The genes encoding for the ventricular myocardium isoforms of myosin light chains were analysed for HCM causal mutations in the present study and, therefore, will be considered in detail later in this chapter.

The actin- and ATP-binding sites are crucial for the myosin function. During contraction, the myosin heads attach to actin, forming so called "cross-bridges" between the thick and thin filaments. Subsequently, an ATP molecule binds up to a myosin head. Following ATP hydrolysis along with the release of products of this hydrolysis causes conformational changes in the myosin heads, which result in the displacement of the thin filament along the thick filament causing contraction.

The force generating myosin-actin interaction is regulated by tropomyosin, the troponin complex, and calcium ions.<sup>23</sup> In a relaxed muscle, tropomyosin, troponin T and troponin I inhibit the attachment of the myosin heads to actin. With the beginning of a contraction event, myoplasmic  $\text{Ca}^{2+}$  concentration increases from  $10^{-7}$  to about  $10^{-5}$  M. Troponin C subsequently binds up to four calcium ions and relieves the inhibition of the actin-myosin interaction produced by tropomyosin, troponin T and troponin I. This enables the myosin heads to form cross-bridges and to draw the actin filament towards the centre of the sarcomere. Cycling formation of cross-bridges occurs until myoplasmic concentration of  $\text{Ca}^{2+}$  decreases, and troponin C relieves the  $\text{Ca}^{2+}$  molecules bound to it.

The mechanisms by which sarcomeric protein mutations lead to HCM are still unclear. However, the evidences accumulated from diverse functional studies, including animal modelling, have led to a hypothesis, which considers myocyte disarray, hypertrophy and interstitial fibrosis as a compensatory response to the alteration of the sarcomere contractile function by mutated proteins.<sup>3,24</sup> In the case of missense mutations, it is assumed that mutated proteins are incorporated into the myofibrils and act as "poison peptides" affecting the function of the normal proteins (dominant-negative effect). Truncation mutations are assumed to result in an insufficient amount of functional proteins by either complete inactivation of a mutated allele or production of truncated proteins unable to incorporate into the myofibrils ("haploinsufficiency" or "null



allele" effect). Both cases lead to the impairment of force generation by the contractile units. The contractile deficit further provides the primary stimulus for increased expression of trophic and mitotic factors in the heart (such as insulin-like growth factor 1, transformic growth factor, and endotelin 1), which leads to hypertrophy, disarray and interstitial fibrosis characteristic of HCM. However, despite already available supporting evidences such as the observation of impaired mechanical performance of cardiac myocytes expressing mutated sarcomeric proteins, decreased LV end-systolic stress-volume ratio, and upregulation of the above stated trophic factors in patients with HCM, more studies are needed to prove the accuracy of this hypothesis.

## 1.2 The ventricular myosin regulatory and essential light chains

The human **MYL2** gene encoding for the ventricular myosin regulatory light chain (**RLC** or also called MLC-2s/v) is located on chromosome 12q23-q24.3.<sup>25</sup> Seven coding exons of this gene encode for a polypeptide of 166 amino acids. Apart from ventricular myocardium, the RLC is also expressed in slow skeletal muscle fibers.

The ventricular myosin essential light chain (**ELC** or MLC-1s/v) is encoded in humans by the **MYL3** gene. It is located on chromosome 3p21.3-p21.2 and is also composed of seven exons, of which the last one is noncoding.<sup>26</sup> **MYL3** encodes for a polypeptide of 195 amino acids, which is, similar to the RLC, expressed in ventricular myocardium and slow skeletal muscle.

The RLC and ELC belong to a family of calcium-binding proteins like calmodulin and troponin C. The common feature of these proteins is the presence of structural motifs made up of a bivalent-cation-binding loop flanked by  $\alpha$ -helices. These motifs are also called EF-hand domains. Calmodulin and troponin C have four functionally active EF-hand domains, which are essential for striated and smooth muscle contraction.<sup>23,27</sup> It has been shown that deletions and non-conserved amino acid substitutions inactivate all EF-hand domains of the ELC and three of the RLC.<sup>28</sup> Only one N terminal EF-hand domain of the RLC retains the ability to bind a bivalent cation.<sup>28</sup>

Besides the EF-hand domain, the RLC possesses a putative phosphorylation site on a single serine residue at the amino termini (Ser15),<sup>29</sup> while the ELC has an actin-binding site also at its amino terminal half.<sup>30</sup>

The function of myosin light chains in striated muscle is only partially understood. Based on the three-dimensional structure, it has been initially suggested that a major function of the striated muscle myosin light chains is to stabilize and elongate the 8.5 nm  $\alpha$ -helical neck region of myosin.<sup>21</sup> It is thought that a swinging motion of this neck relative to the catalytic domain is essential in amplifying generated power stroke (the lever arm model).<sup>21,31</sup> Further functional studies, however, have suggested that the striated muscle myosin light chains also regulate and modulate the myosin-actin interaction.<sup>30,32-34</sup>

The ELC is thought to modulate the force production by binding with its N-terminus to the C-terminus domain of actin and thereby acting as a tether between the thin and thick filaments.<sup>30</sup>

The RLC might influence the myosin-actin interaction through phosphorylation and/or calcium binding. It was shown that RLC phosphorylation increases the rate of cross-bridges and, hence, increases the force production in cardiac and skeletal muscles at low levels of calcium.<sup>35,36</sup> The mechanism of such effects of RLC phosphorylation might involve the conformational change of the entire myosin head due to a change in the charge of the N-terminal region of the RLC that occurs upon phosphorylation.<sup>37,38</sup>

It was also shown that a definite link exists between RLC phosphorylation and calcium binding.<sup>29,39</sup> Szczesna *et al.*<sup>39</sup> demonstrated that inactivation of the RLC calcium-binding site causes removal of all effects of phosphorylation. Furthermore, both phosphorylation and calcium binding properties as well as their relationship have been shown to be altered due to HCM-causing RLC mutations suggesting that alteration of exactly these properties could contribute to the pathogenesis of this disorder.<sup>29</sup>

### 1.3 Clinical features and diagnosis of HCM

HCM is a clinically heterogeneous and unpredictable disease. Its clinical manifestations vary from a benign course to that of severe heart failure and peripheral embolisation.<sup>5</sup> The importance of recognising this disorder in patients as early as possible is highlighted by a high rate of sudden cardiac death in young people.

Premature death can occur even in completely asymptomatic patients as the first manifestation of the disease.

Myocardial hypertrophy generally develops during adolescence, however, in severe cases it can occur in an infant or even during foetal life. Simultaneously with hypertrophy, some HCM patients become symptomatic, while others exhibit no symptoms over long periods. HCM patients generally present with dyspnea, angina pectoris, palpitations, fatigue, presyncope, and syncope. Although these symptoms are common in all HCM patients, their onset and severity show great variability.

In approximately 25% of cases, myocardial hypertrophy leads to dynamic LV outflow or midventricular obstruction and, consequently, to the development of a pressure gradient.<sup>40</sup> In case of LV outflow tract obstruction, apart from hypertrophy, systolic anterior motion of the mitral valve and mitral valve-septal contact contribute to the development of the pressure gradient. The value of the pressure gradient varies among the patients. If pressure gradients of >30 mm Hg (at rest) are present, the potential for further hypertrophy and deterioration is very likely.<sup>40</sup> In such patients, operative reduction of the pressure gradient by means of septal myectomy (Morrow procedure) or nonsurgical septal reduction has been shown to be effective.<sup>40</sup> Patients with the obstructive form of HCM usually exhibit a number of clinical signs, which are not seen in the non-obstructive form of the disease. Among them are systolic ejection murmur, bifid arterial pulse, double systolic impulse, and paradoxically split second heart sound.<sup>41</sup>

The minimal investigations needed for the diagnosis of HCM include ECG and transthoracic echo Doppler examination. Electrocardiogram is generally abnormal in HCM, although entirely normal electrocardiograms are seen in about 15% of patients and usually are found in the presence of only localized LV hypertrophy.<sup>42</sup> The most common abnormalities are evidence of LV hypertrophy, negative T-waves, ST abnormalities, and pathological Q-waves. All these abnormalities can be absent in children and become evident over time with development of LV hypertrophy. However in some cases, especially in the young, ECG may be abnormal, even when echocardiography reveals no LV hypertrophy.<sup>43</sup>

Transthoracic echo Doppler examination is the most important diagnostic test in HCM. These combined techniques allow the assessment of extent and distribution of hypertrophy, systolic and diastolic function, the presence of systolic anterior motion of mitral valve, and the severity of the pressure gradient. The magnitude of LV wall

thickness can be very variable (13 - 30 mm or more).<sup>44</sup> The location of hypertrophy is also diverse, although four frequent patterns of LV hypertrophy distribution have been reported.<sup>45</sup> Type I is confined to the anterior portion of the interventricular septum (IVS), whereas type II involves the entire IVS. Type III, the most common, is characterized by hypertrophy of substantial portions of both interventricular septum and LV anterolateral free wall. Hypertrophy identified in regions of the LV other than basal IVS belongs to type IV.

Among other investigations, Holter ECG monitoring is a valuable tool in assessing the type and severity of cardiac arrhythmias. Chest X-ray, heart catheterisation, and magnetic resonance imaging can be helpful in the differential diagnosis of HCM, revealing the particular hypertrophy pattern and the stage of congestive heart failure.

Clinical heterogeneity of HCM makes it difficult to predict the outcome of the disease and to diagnose subjects who are in a high risk of premature death. According to clinical studies, a family history of premature sudden cardiac deaths, magnitude of hypertrophy more than 30 mm, an abnormal blood pressure response to exercise testing, and nonsustained/sustained ventricular tachycardia could be used as markers for sudden cardiac death in HCM and justify prophylactic therapy with amiodaron or implantation of cardioverter defibrillator.<sup>44,46,47</sup> However, the accuracy of these risk factors is still subject of discussion. For instance, it has been argued that such risk factor as magnitude of hypertrophy is not accurate, since sudden cardiac death also occurs in the presence of little hypertrophy as in HCM caused by mutations in cardiac troponin T.<sup>48,49</sup> A recent study showed that combination of the several risk factors increases the likelihood of sudden death.<sup>46</sup> In addition to the investigation of the clinical risk factors, attempts have also been directed towards establishing genetic markers for assessing the severity of HCM phenotypes.

## 1.4 Genotype-phenotype correlation studies

Genotype-phenotype correlation studies have revealed that HCM phenotype is substantially influenced by the nature of the causative genetic defect. The causal gene as well as the type and localization of a mutation play the primary role. Thus, mutations in the  $\beta$ -myosin heavy chain gene are generally associated with more significant hypertrophy and severe disease course than those in the other genes.<sup>50,51</sup> Myosin binding protein-C gene mutations are mostly characterized by late clinical manifestation and a relatively benign disease course.<sup>52</sup> High incidences of sudden cardiac death but little LV hypertrophy are features of cardiac troponin T mutations.<sup>53</sup> Mutations in the cardiac troponin I gene have been shown to cause LV apical hypertrophy,<sup>11</sup> whereas those in the ventricular myosin light chain genes have been initially associated with left midventricular hypertrophy.<sup>10</sup> Concerning the causal mutations, protein truncation mutations or those located in highly important protein domains are generally associated with a severe course of HCM.<sup>54,55</sup>

The diversity in disease appearance in individuals bearing exactly the same mutation suggested that phenotypic expression of HCM is also influenced by factors other than the basic genetic defect, such as modifier genes or environmental influences.<sup>56</sup> Amongst the known potential modifier genes are those encoding for functional variants of angiotensin-1 converting enzyme, angiotensinogen, endothelin-1, and several trophic factors.<sup>3,57</sup>

Correlation studies have also revealed that causal mutations carry prognostic significance.<sup>58</sup> Some of them were associated with poor prognosis and a high incidence of sudden cardiac death and could be therefore used as genetic markers for sudden death in HCM. Table 1.2 lists some mutations associated with a high, intermediary and low risk of sudden cardiac death in HCM.

**Table 1.2.** Mutations and prognosis in HCM

Sarcomeric protein	Prognosis		
	Good	Intermediate	Poor
$\beta$ -MHC	Gly256Glu	Arg249Gln	Arg403Gln
	Leu908Val	Glu930Lys	Arg719Trp
	Val606Met	Val606Met	Arg453Cys
	Phe513Cys		Arg723Gly
	Asn232Ser		
Cardiac troponin T	Ser179Phe	Phe110Ile	Arg92Gln
			Arg92Trp
			Ile79Asn
			delGlu160
			Ser179Phe (homozygous)
MYBP-C	All unless listed	SASint20*	
$\alpha$ -Tropomyosin	Asp175Asn		
<b>Myosin light chains</b>		<b>Insufficient data</b>	

Note:  $\beta$ -MHC,  $\beta$ -myosin heavy chain; MyBP-C, myosin binding protein-C. \*Splice acceptor site mutation in intron 20. From ref. 58.

One should also keep in mind that the number of families identified with each specific mutation is relatively small, and the described phenotypes may be unique to the particular family and not generally applicable. More studies are needed to draw strong and accurate conclusions regarding the prognostic significance of a given genetic defect. However, identification of a malignant mutation along with the clinical risk factors can be useful in revealing patients with an adverse disease phenotype and the need for preventive measures.

## 1.5 Aims of the present study

In comparison with other disease genes, only few studies concerning the *MYL2* and *MYL3* genes have been performed so far. As mentioned above, mutations in these genes have been initially associated with a particular phenotype with massive hypertrophy of papillary muscles and adjacent LV tissue causing midventricular obstruction.<sup>10</sup> However, further investigations have shown that typical septal hypertrophy can be also caused by ELC and RLC mutations.<sup>15,16,59</sup> In contrast to other genes, phenotypic characterisation of HCM caused by defects in *MYL2* and *MYL3* has mainly dealt with the pattern of hypertrophy, and very little data are available regarding the disease course and prognosis.

Considering the limited information on HCM related to the ELC/RLC, this study was aimed to detect disease-causing mutations in the *MYL2* and *MYL3* genes in a group of clinically well-characterized HCM patients. Further purpose was to assess whether the detected mutations are associated with malignant or benign phenotype in the respective families.

## 2 Materials and methods

### 2.1 Clinical evaluation

A total of 71 unrelated HCM patients were consecutively enrolled from Charité/Franz-Volhard-Klinik (Berlin, Germany), the National Center of Cardiology and Internal Medicine (Bishkek, Kyrgyzstan), Hospital Pulido Valente (Lisbon, Portugal) and Klinik für Thorax- und kardiovaskuläre Chirurgie (Düsseldorf, Germany). Informed consent was obtained in accordance with the guidelines of institutional ethic commissions. Clinical evaluation was performed on the basis of medical history, physical examination, 12-lead electrocardiogram, M/B-mode and Doppler echocardiography, and, in some cases, Holter electrocardiography. The echocardiographic evaluation was performed without prior knowledge of genetic results according to the guidelines of the American Society of Echocardiography.<sup>60</sup> Left ventricular (LV) wall thickness of  $\geq 13$  mm<sup>43</sup> was used as the inclusion criterion in the absence of other known causes for LV hypertrophy (hypertension, aortic stenosis, etc).

Once the mutations were identified in probands, members of family K and B were invited to undergo genetic analysis and clinical evaluation. The clinical diagnosis of HCM in participating family members was based on the presence of LV hypertrophy observed by echocardiography and corrected to age, weight and body surface area according to Henry *et al.*<sup>61</sup>

Blood samples were drawn from all HCM patients and family members in tubes containing 1.6 mg/ml EDTA and stored at -20 °C until DNA extraction. Blood for control DNA was obtained from anonymous blood donors.

Statistical analysis was performed using StatView software, release 4.51, PowerPC Version (Abacus Concepts Inc, Berkeley, California). Data are expressed as the mean value  $\pm$  standard deviation or number (%) of patients.



## 2.2 Genetic analysis

### 2.2.1 Approach overview

The approach undertaken in the present study allows performing genome screening for unknown mutations in a large patient group. The screening started with the isolation of total genomic DNA from blood of patients. Genomic DNA was used thereafter as a template for amplifying a gene of interest by means of polymerase chain reaction (PCR). All amplified fragments were screened further by single strand conformation polymorphism (SSCP) analysis. Samples showing an aberrant band pattern on SSCP gels were selected for direct automated DNA sequencing for detection of possible mutations. Once a mutation was identified, it was confirmed by another sequencing run or, when possible, by restriction fragment length polymorphisms analysis. The latter was also used for screening family members for the identified mutation (figure 2.1).

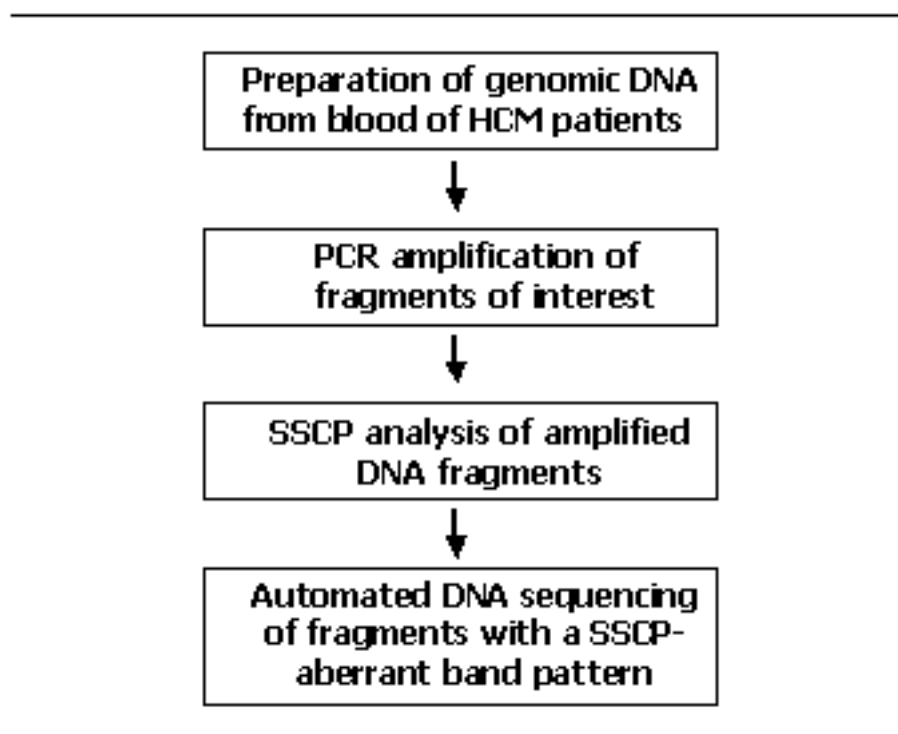


**Figure 2.1. Schematic representation of the approach for mutation detection undertaken in the present study.** DNA, deoxyribose nucleic acid; PCR, polymerase chain reaction; SSCP, single strand conformation polymorphism.

### 2.2.2 Preparation of genomic DNA

Genomic DNA was isolated from peripheral blood obtained from patients and stored at -20 °C. A modified DNA extraction method suggested by Lahiri and co-workers was used.<sup>62</sup> It yields up to 150 µg of DNA from 5 ml of blood. An advantage of this method is that it avoids the use of any toxic organic solvents required for elimination of cellular proteins. Unlike other standard techniques, these proteins are removed by using saturated sodium chloride solution. Moreover, the method eliminates the step of prolonged digestion of samples with proteinase K, thus saving costs and time.<sup>62</sup>

The following protocol was used:

1. 5 ml of blood sample, 5 ml of low salt buffer TKM1 (10 mM Tris, pH 7.6; 10 mM MgCl<sub>2</sub>, and 2 mM EDTA) and 100 µl of triton X-100 were mixed and centrifuged at 2500 rpm for 20 min. The supernatant was poured off.
2. 5 ml of the TKM1 buffer was added to the pellet and followed by centrifugation at 2500 rpm for 20 min; supernatant was then poured off. This step was repeated at least two times more.
3. The saved pellet was resuspended in 800 µl of high salt buffer TKM2 (10 mM Tris, pH 7.6; 10mM KCl; 10 mM MgCl<sub>2</sub>; 0.4 mM NaCl, and 2 mM EDTA) and 50 µl of 10% SDS, mixed and incubated at 55° C for 10 min in a water bath.
4. 100 µl of 5 M NaCl was pipetted in the tube, mixed and centrifuged at 1200 rpm for 5 min. The supernatant containing DNA (about 1 ml) was transferred into a new tube, mixed with two volumes of absolute ethanol (about 2 ml) at room temperature; the tube was then inverted several times until DNA precipitated.
5. The DNA was further transferred in a new tube containing 1 ml of ice-cold 70% ethanol and centrifuged for 5 min at 1200 rpm at 4 °C. The DNA containing pellet was dried of rest of ethanol for 10 min in a vacuum centrifuge and then resuspended in 500 µl of Tris buffer (10 mM, pH 8.0) at 65 °C for 15 min and used further as DNA stock solution.

The quality of extracted DNA was assessed by agarose gel electrophoresis. Concentration of DNA in the stock solution was determined by measuring the absorption at 260 nm (1 absorbance unit corresponds to 50 µg/ml) in the Ultrospec Plus spectrophotometer (Pharmacia). Working solution containing 25 ng/µl of genomic DNA was diluted from the stock solution adding respective volume of Tris buffer (10 mM, pH 8.0). The stock solution was stored at -20 °C, whereas the working solution was further used for PCR.

### **2.2.3 Amplification of coding exons of *MYL2* and *MYL3***

The polymerase chain reaction (PCR) is one of the most rapid *in vitro* methods for producing large quantities of a particular DNA region for further molecular analysis. It is based on the extension of two recombinant oligonucleotide primers, each complementary to the opposite DNA strands and flanking the region of interest. The extension is carried out by a recombinant DNA polymerase in the presence of deoxynucleotides (dNTPs) and buffer containing magnesium. Specially designed PCR thermo cyclers allow rapid changing and repeating of different temperatures required for DNA denaturing, primer annealing and extension.

PCR primers were designed on the basis of *MYL2* and *MYL3* reference genomic DNA sequences downloaded from GenBank ([www.ncbi.nlm.nih.gov](http://www.ncbi.nlm.nih.gov)). GenBank accession numbers for the *MYL2* and *MYL3* reference sequences are L01652 and J04462, respectively. Forward and reverse primers were designed for each of the seven coding exons of *MYL2* and six coding exons of *MYL3* using OLIGO software, release 4.06 (National Biosciences, Inc, Plymouth, USA). The primers are listed in table 2.1.

**Table 2.1.** Oligonucleotide primers used to amplify coding exons of *MYL2* and *MYL3*

Gene	Exon	Forward primer	Reverse primer
<i>MYL2</i>	1	5'ACCTATGACTGCCAAAAGCG3'	5'GTAGTGGCTTCCTCTCCTCG3'
	2	5'GGGGCCTGACCTAGTTTTT3'	5'TTTGGGATTGTTTGGAGGAT3'
	3	5'TCCACTCCTGCCAACTCCTT3'	5'ACCCACCTCCTGCTCCTCAT3'
	4	5'GCCTCATCACCCCATCTCTG3'	5'AGCCCCCCCCGAAGAAACATA3'
	5	5'TCATCTCTGGGGGAAGTTGG3'	5'TGTGTGTGTGTAGGGGGG AC3'
	6	5'AAAGGGGTGCTGAAGGCTGA3'	5'AGACGAGAGGGGAGACGGAG3'
	7(A)	5'TCCGTCTCAGTTCCCTCCC3'	5'GTACCCATAGCCACCCAGGC3'
	7(B)	5'GCCCCATTTATCCACCTCCA3'	5'GGCTTTGGTCATCCAGGTAA3'
<i>MYL3</i>	1	5'GGGGTCATGAGGTATCCGGG3'	5'TCCACTCACTTGCCCTGCTC3'
	2	5'CCACCTTTTAAGCCGGGCAT3'	5'CCGCAGGACATCCCCACACT3'
	3	5'ATTGAAGGTGAGCAGGGGTC3'	5'TAACACTATGGGGGCTCTCG3'
	4	5'GTGTGAGAGGTGGGGATAGC3'	5'TGGAAGGAGTTGGGGTAGGG3'
	5	5 TGA CT CAG CCT CCC ACT CCT 3'	5'CTCCCCTCCCAGAAGACCCC3'
	6	5'GGTCTTCTGGGAGGGGAGTG3'	5'TTCCCTGGGCTTCCTGAGAG3'

Each primer was 20 base pairs (bp) in length. Most PCR products were 150-400 bp long, which is in an optimal range for SSCP analysis and DNA sequencing. Exon 7 of *MYL2* was divided into two parts, and a primer pair was determined for each part. Primers were located in the exon-flanking intronic region not closer than 30 base pairs to the start/end of exon. This allowed good reading of the sequence of the whole exon. DNA sequencing was performed by the Dye Primer Chemistry method, which requires specific oligonucleotide sequences to be incorporated in a PCR product. This was achieved by attaching the required sequences to 5'-end of primers. The 21-M13 sequence (5'-TGTAAGGAGGGCCAGT-3') was attached to each forward primer, whereas the M-13 sequence (5'-CAGGAAACAGCTATGACC-3') was connected to each reverse primer. The primers were produced by BioTeZ.

After obtaining the primers, a PCR protocol was optimised for each exon in terms of primer concentration, primer specific annealing temperature, and number of cycles. Final values are listed in table 2.2.

**Table 2.2.** Optimised parameters of PCR protocols used to amplify coding exons of *MYL2* and *MYL3*

Gene	Exon	Primer concentration pmoles/ $\mu$ l	Annealing temperature $^{\circ}$ C	Number of cycles
<i>MYL2</i>	1	0.125	60	38
	2	0.125	59	40
	3	0.2	57	34
	4	0.16	57	34
	5	0.125	63	35
	6	0.125	63	35
	7A	0.2	59	31
	7B	0.4	57	35
<i>MYL3</i>	1	0.08	54	32
	2	0.08	63	34
	3	0.125	63	34
	4	0.08	63	34
	5	0.16	63	29
	6	1.125	61	32

Note: concentration of forward and reverse primers was identical and calculated for one sample.

The concentration of the required reagents other than primers, *i.e.* PCR buffer,  $\text{MgCl}_2$ , dNTPs, AmpliTaq DNA polymerase and genomic DNA, was identical for all exons (table 2.3). A PCR mix of final volume of 25 or 38  $\mu$ l was used. Composition of the reaction mix for amplifying one sample is shown in table 2.3.

**Table 2.3.** Composition of 25  $\mu$ l PCR mix for one sample

Reagent, company	<i>MYL2</i>			<i>MYL3</i>		
	ex 1,2,5,6	ex 3,7A	ex 4	ex 1,2,4	ex 3,6	ex 5
	end vol, $\mu$ l	end vol, $\mu$ l	end vol, $\mu$ l	end vol, $\mu$ l	end vol, $\mu$ l	end vol, $\mu$ l
Deionized water	18,2	17,4	17,8	18,2	18,2	17,8
10xPCR buffer, Appl Bios	2,5	2,5	2,5	2,5	2,5	2,5
$\text{MgCl}_2$ , 25 mM, Appl Bios	1,5	1,5	1,5	1,5	1,5	1,5
Forward pr, 5 pmoles/ $\mu$ l, BioTeZ	0,6	1	0,8	0,4	0,6	0,8
Reverse pr, 5 pmoles/ $\mu$ l, BioTeZ	0,6	1	0,8	0,4	0,6	0,8
dNTP, 20 mM, ByoZym	0,3	0,3	0,3	0,3	0,3	0,3
Amplitaq, 5 U/ $\mu$ l, Appl Bios	0,3	0,3	0,3	0,3	0,3	0,3
DNA, 25 ng/ $\mu$ l	1	1	1	1	1	1

Abbreviations used in the table: ex, exon; Appl Bios, Applied Biosystems; Forward pr, forward primer; Reverse pr, reverse primer; dNTP, deoxynucleotides; end vol, end volume

All PCR reagents were mixed together in a 0.2 µl PCR tube, which was then placed in a thermal cycler (Peltier Thermal Cycler, MJ Research Inc; Uno-Thermoblock, Biometra). The following cycling programme was used:

I. Initial denaturing	90 °C	2 min
	94 °C	1min
II. 29 -40 cycles for		
annealing	Primer specific annealing temperature (57 - 63 °C)*	15 sec
extension	72 °C	2 min
denaturation	92 °C	30 sec
III. Final annealing	Primer specific annealing temperature (57 - 63 °C)*	15 sec
IV. Final extension	72 °C	10 min

\*Primer specific annealing temperatures are listed in table 2.2.

The quality of obtained PCR products was assessed by agarose gel electrophoresis.

#### 2.2.4 Single strand conformation polymorphism analysis

Single strand conformation polymorphism (SSCP) analysis is a widely used method for carrying out efficient and economical screening for unknown mutations in the PCR amplified region of interest in the genome. The sensitivity of SSCP analysis has been shown to be about 80-90% if fragments are shorter than 400 bp and if optimal running conditions are used.<sup>63,64</sup> The method is based on assessment of mobility of a single DNA strand by non-denaturing polyacrylamide gel electrophoresis. Amplified fragments are thermally denatured and rapidly cooled. This results in single DNA strands, which refold in specific conformations unique to the nucleotide sequence. In comparison with wild type, a mutated DNA strand adopts different conformations and, consequently, migrates differently when subjected to electrophoresis. On a stained SSCP gel, such mobility shift can be recognized as an aberrant band pattern. Generally, aberrant band patterns are characterized by the presence of additional bands in comparison with neighbouring patterns. Samples showing an aberrant pattern are selected for further sequence analysis.

In the present study, experimental conditions were optimised for each PCR amplified fragment. Two different conditions with respect to gel composition and running temperature were used to test each sample (table 2.4).

**Table 2.4.** SSCP conditions used to screen *MYL2* and *MYL3*

	<i>MYL2</i>			<i>MYL3</i>			
	ex 1- 6	ex 7A	ex 7B	ex 1,3,6	ex 2	ex 4	ex 5
<b>Condition I</b>							
Gel type	MDE	MDE	MDE	MDE	MDE	MDE	MDE
Temperature, °C	5	5	20	20	20	25	5
Run duration, min	75	75	75	120	120	120	80
<b>Condition II</b>							
Gel type	MDE	MDE-F5%	MDE-F10%	MDE	6% PAA	6% PAA	MDE
Temperature, °C	10	20	10	25	17	25	10
Run duration, min	75	75	75	120	100	100	80

Abbreviations used in the table: ex, exon; MDE, Mutation Detection Enhancement gel; MDE-F5%, 2XMDE gel containing 5% of Formamide; 2xMDE-F10%, 2XMDE gel containing 10% of Formamide; 6% PAA, 6% polyacrylamide gel.

As shown in table 2.4, four different modifications of polyacrylamide gel were used. The Mutation Detection Enhancement (MDE) gel solution is a polyacrylamide matrix that has a high sensitivity to DNA conformational differences. This ready to use solution was purchased from BioWhittaker Molecular Application. MDE gels were used for screening most of the exons. In two exons of *MYL2*, MDE gels were modified by addition of 5% and 10% of formamide. In two exons of *MYL3*, 6% acrylamide gel was prepared from a Rotiphorese gel 29:1 ready to use solution (acrylamide/bisacrylamide in ratio 29:1), which was purchased from Roth. Composition of these gels is given in table 2.5.

**Table 2.5.** Composition of SSCP gels used to screen *MYL2* and *MYL3*

Gel name	Compounds	Quantity, ml
MDE	2xMDE solution	7.5
	10xTBE buffer	1.8
	Deionized water	20.8
MDE-F5%	2xMDE solution	7.5
	10xTBE buffer	1.8
	Formamide	1.5
	Deionized water	19.3
MDE-F10%	2xMDE solution	7.5
	10xTBE buffer	1.8
	Formamide	3.0
	Deionized water	17.8
6% PAA	Rotiphorese gel 29:1	4.7
	10xTBE buffer	1.8
	Deionized water	20.8

Note: 10xTBE buffer contained 450 mM Tris, 450 mM Boric acid, 20 mM EDTA.

An apparatus for casting a SSCP gel consisted of two glass plates sized 26 x20 cm (Amersham Bioscience). One of the plates was coated with 0.5 mm thick and 5 mm broad rubber around the side and foot edges and had a row of 26 small slots. Special firm plastic foil (Serva) was put between the glass plates and used for gel backing. SSCP gel compounds (see table 2.5) were mixed in a glass beaker. Immediately after adding 24 µl of 99% TEMED and 48 µl of 40% ammonium persulfate, a gel was cast in the space between the foil and the rubber-coated plate and polymerised for 1-2 hours.

The PCR products were mixed with equal or double volume of formamide loading buffer (formamide 0.9 g/ml, 10 mM NaOH, 11mM EDTA), denatured at 95 °C for 3 min and quenched on ice for 1 min prior to loading. 8 µl of diluted samples were loaded onto the polymerised gel, which was previously taken out of the glass plates and placed in electrophoresis unit Multiphor II (Pharmacia). The gel was run at 35 Volt and at corresponding temperatures (table 2.4). After electrophoresis, bands on the gel were visualized by silver staining according to a protocol adapted from Pharmacia (table 2.6).

**Table 2.6.** Silver staining protocol used to visualize DNA on a SSCP gel

Step	Solutions	Time
Fixation	Acetic acid glacial 25 ml Make up to 250 ml with deionized water	20 min
Washing	Deionized water	3x2 min
Silver reaction	1% silver nitrate solution 25 ml 37% formaldehyde 0.25 ml Make up to 250 ml with deionized water	20 min
Washing	Deionized water	0.5 min
Developing	Sodium carbonate 6.25 g 37% formaldehyde 0.25 ml 2% Sodium thiosulphate 0.25 ml Make up to 250 ml with deionized water	until bands become visible
Stopping	Glycin 5 g 0.5 M EDTA 18.8 ml Make up to 250 ml with deionized water	10 min
Preserving	99.5% glycerol 25 ml Make up to 250 ml with deionized water	10 min

After silver staining, the gel was transferred onto another glass plate, covered with thin soft plastic foil (Cotech) and fixed by tape. The gel was dried for 24-48 hours, removed from the plate and evaluated. Samples showing an aberrant pattern were



selected and subjected to direct automated DNA sequencing for detection of possible mutations.

### 2.2.5 Automated DNA sequencing

Direct genomic DNA sequencing was performed using the Dye Primer Chemistry method on a 373 DNA sequencing system (Applied Biosystems). The method employs four specific sequencing primers labelled with one of four fluorescent tags (JOE, FAM, TAMRA, ROX) corresponding to the four nucleotides. Using a PCR amplified DNA fragment as a template, each primer is extended in a separate tube in the presence of corresponding dideoxynucleotides and deoxynucleotides as well as DNA polymerase and specific buffer. In each tube, cycle sequencing reaction produces fluorescently labelled, chain-terminated DNA fragments. The contents of all four tubes are pooled together after cycle sequencing and loaded in a single lane on a denaturing gel. During electrophoresis, the labelled fragments pass through a laser beam, directed near the bottom of the gel, which excites the fluorescent tags. The emitted light is then detected by a photomultiplier and directed into a computer, which displays the readout as series of four different coloured peaks, one colour for each nucleotide.

The Dye Primer Chemistry kits for cycle sequencing were purchased from Applied Biosystems. In order to sequence both the sense and antisense DNA strands, two kits containing either forward or reverse primers were used. Each kit included four different ready to use mixes (A-, C-, G-, T-mix) corresponding to each of the four nucleotides (table 2.7).

**Table 2.7.** Components of Dye Primer Chemistry kit

Ready Reaction Mix Reagents	
A-mix	ddATP, forward/reverse JOE dye primer
C-mix	ddCTP, forward/reverse FAM dye primer
G-mix	ddGTP, forward/reverse TAMRA dye primer
T-mix	ddTTP, forward/reverse ROX dye primer
All mixes	dATP, dCTP, 7-deaza-dGTP, dTTP, Tris-HCl (pH 9.0 at 25 °C), MgCl <sub>2</sub> , thermall stable pyrophosph

Apart from samples with an aberrant band pattern on SSCP gels, two HCM samples with a normal band pattern were sequenced for each exon of *MYL2* and *MYL3*. Control DNA was sequenced when needed.

PCR products were mixed with the ready reaction mixes in four 0.2 µl tubes in following proportions:

Reagent	A, µl	C, µl	G, µl	T, µl
Ready reaction mix	4	4	8	8
PCR product	1	1	2	2
Total volume	5	5	10	10

After brief centrifugation, tubes were put in a thermal cycler pre-heated at 94 °C. The following programme was used:

I. 15 cycles of	96 °C	10 sec
	55 °C	5 sec
	70 °C	60 sec
II. 15 cycles of	96 °C	10 sec
	70 °C	60 sec

After cycle sequencing, contents of the four tubes were centrifuged and pooled together in a 2.0 ml tube already containing 80 µl of 95% ethanol and 1 µl of 2% blue dextran. The sample was further placed on ice for 15 min and thereafter centrifuged for 30 min at 1200 rpm at 4 °C. The supernatant was then poured off, and pellet was dried of rest of ethanol for 10 min in a vacuum centrifuge. For loading, the pellet was resuspended in 3.5 µl of formamide loading buffer (deionised formamide and EDTA/5 % blue dextran in ratio 5:1) or stored at -20 °C, when it was not loaded on the gel the same day.

A 0.3 mm thick sequencing gel was cast between two glass plates sized 25x59 cm (Applied Biosystems) previously washed with 1%alconox solution and cleaned with 70% ethanol. The gel composed of 30 g urea, 10 ml of 30% acrylamide solution, 6 ml of 10xTBE buffer (450 mM Tris pH 8.0, 450 mM boric acid, 20 mM EDTA) and 22 ml of deionized water. 15 µl of 99% TEMED and 350 µl of 10% ammonium persulfate were added to the gel briefly before pouring in. The gel was poured in between the glass plates with the aid of a 50 ml syringe and polymerised for 2 hours.

The resuspended pellet (see above) was denatured at 95 °C for 3 min and loaded onto the gel. The gel was run for 15 hours at 2500 Volt. The generated sequences were stored and further analysed manually and by using the Sequencher software, release 4.1, PowerPC Version (Gene Codes Corporation, USA), which facilitated comparison of generated sequences to the corresponding reference sequences obtained from GenBank.

### 2.2.6 Restriction fragment length polymorphism analysis

Restriction fragment length polymorphism (RFLP) analysis is a method of detecting known mutations by digestion of DNA fragment with a restriction enzyme. In the present study, this method was used to confirm the presence of mutations initially identified on sequencing as well as to screen for it in family members. The method is more rapid and less time consuming when compared to sequencing, but it is possible only when restriction enzyme recognition sequence is affected by a mutation. Some mutations remove existing recognition sites of an enzyme, whereas others introduce new ones. In both cases, the presence of a mutation is recognized by observation of particularly sized restriction fragments.

Screening for the Glu22Lys mutation in exon 2 of *MYL2* within family K and controls was done by digestion with the *Taq*<sup>α</sup> I restriction enzyme (New England Biolabs). 4 µl of amplified fragments were mixed with 4 Units (0.2 µl) of *Taq*<sup>α</sup> I, 1 µl of 10xNEB buffer, 1 µl of 10xBSA, and 3.8 µl of deionized water. The samples were then incubated at 65 °C for 2 hours in a thermal cycler.

The *Sty* I restriction enzyme (New England Biolabs, USA) was used to confirm the c.169C>G variant in exon 3 of *MYL2*. 4 µl of amplified fragments were mixed with 5 Units (0.5 µl) of *Sty* I, 1 µl of NEBuffer, 1 µl of 10xBSA, and 3.5 µl of deionized water. The samples were then incubated at 37 °C for 2 hours in a thermal cycler.

The digested products were separated on a 4% agarose gel and stained with ethidium bromide.

### 2.2.7 Agarose gel electrophoresis

Agarose gel electrophoresis was used for assessing the quality of genomic DNA and amplified PCR products as well as for separating products of RFLP analysis. A 1.5% agarose gel was used to check the quality of genomic DNA after it was extracted from blood, whereas a 4% agarose gel was used for loading PCR amplified fragments and restriction enzyme digests (table 2.8). DNA was stained with ethidium bromide added into a gel and visualized under UV light on Transilluminator TI 1 (Biometra).

**Table 2.8.** Agarose gel composition

	1% gel	4% gel
Agarose, g	0.3	0.8
1xTBE, ml	20	20
1% Ethidium bromide, $\mu$ l	1.5	1.5

Note: 1xTBE buffer contained 45 mM Tris (pH 8.0), 45 mM Boric acid and 2 mM EDTA.

Agarose powder was mixed with 1xTBE buffer and boiled in a microwave until agarose melted completely. 1.5  $\mu$ l of ethidium bromide was added into the solution, and it was briefly boiled again. The gel was poured into a horizontal apparatus (GibcoBRL) and polymerised for 20 min. The apparatus was then filled with 1xTBE buffer until it covered completely the gel and appropriate amount of a sample was loaded onto the gel. Loading volume was 2  $\mu$ l, 3  $\mu$ l, and 10  $\mu$ l for genomic DNA, PCR products, and restriction fragments, respectively. 25 base pair and VIII-DNA molecular weight markers (Roche and GibcoBRL) were used to estimate fragment size of amplified and digested products.

## 2.3 Devices and Chemicals

### 2.3.1 Devices

373 DNA Sequencer	Applied Biosystems
Centrifuge 3K12	Sigma
Centrifuge 3K30	Sigma
Centrifuge RC 5B	Sorvall
Electrophoresis unit Multiphor II	Pharmacia
Enhanced Analysis System 429K	Herolab
Eppendorf Thermomixer 5436/5437	Eppendorf
Horizon 58 Gel electrophoresis Apparatus	GibcoBRL
Ice machine AF - 100	Scotsman
Metallblock-Thermostate DB-3D	Techne
Microwave Micromat	AEG
OPTILAB-Plus-System	MembraPure
Pelitier Thermal Cycler, PTC - 100	MJ Research, Inc
Pelitier Thermal Cycler, PTC - 200	MJ Research, Inc
pH – Meter Calimatic	Knick
Power supply Power Pack P 25	Biometra
Power supply Power Pack ST 606	GibcoBRL
Power supply PS 9009 TC	GibcoBRL
Spectrophotometer Ultrospec Plus	Pharmacia LKB
Thermal cycler Uno-Thermoblock	Biometra
Thermostate Multitemp II/III	Pharmacia
Transilluminator TI 1	Biometra
Vacuum Centrifuge UNIVAPO 150/100	UniEquip
Vacuum pump Cryo Vac	Appligene
Video copy processor	Mitsubishi
Weighing machine Kern 510	Kern

### 2.3.2 Chemicals

Acetic acid (glacial) 100%	Merck
Acetone	Merck
Acrylamide/Bis 29:1	BioRad
Agarose	BioWhittaker Molecular Application
Alconox	Alconox, Inc
Ammonium persulfate	Amresco, Inc
AmpliTaq DNA polymerase	Applied Biosystems
Blue dextran	Pierce
Boric acid	Merck
Bromphenol blue	Pierce
10xBSA buffer	New England Biolabs
dNTPs	ByoZym
Dye Primer Chemistry sequencing kit	Applied Biosystems
Ethanol absolute	Merck
Ethidium bromide	Roth
Ethylenedinitrilotetraacetic acid (EDTA)	Merck
Formaldehyde solution 37%	Merck
Formamide 99.5%	Merck
Glycerol 99.5%	Merck
Glycine	Merck
Hydrochloric acid 32%	Merck
LiChrosolv water for chromatography	Merck
Magnesium chloride	Roth
MDE Solution 2x	BioWhittaker Molecular Application
Mineral oil	Serva
MgCl <sub>2</sub> buffer for PCR	Applied Biosystems
10xNEBuffer	New England Biolabs
PCR-buffer	Applied Biosystems

Potassium chloride	Roth
Rotiphorese gel 29:1	Roth
Silver nitrate	Merck
Sodium carbonate	Merck
Sodium chloride	Roth
Sodium hydroxide pellets	Merck
Sodium thiosulfate pentahydrate	Merck
<i>Sty</i> I restriction enzyme	New England Biolabs
<i>Taq</i> <sup>α</sup> I restriction enzyme	New England Biolabs
TEMED	Promega
Tris (hydroxymethyl) aminomethane	Merck
Triton X-100 99.6%	Calbiochem
Urea	Merck
Xylene cyanol FF	Pierce

## 3 Results

### 3.1 Patient characteristics

A total of 71 unrelated HCM patients including 48 males and 52 females aged 22 - 78 years (mean  $53.3 \pm 14.7$ ) were examined for disease-causing mutations in *MYL2* and *MYL3*. Clinical data on these patients are summarized in table 3.1.

The majority of the patients had either no or mild symptoms (NYHA functional class I and II). Mean interventricular septum (IVS) obtained by echocardiography was  $19.6 \pm 3.7$  mm, while mean left ventricular (LV) posterior wall thickness was  $10.5 \pm 2.4$  mm. LV hypertrophy mostly involved the entire IVS (37% cases of Maron type II) or both IVS and anteriolateral LV free wall (45% of Maron type III).

LV outflow tract obstruction leading to an increased gradient of more than 10 mm Hg between LV and aorta was present in 58 % of the probands. It correlated with the presence of systolic anterior motion of mitral valve (54%). In 8 patients (11%) with the increased outflow tract gradient, an operative management was undertaken. 5 of them (7%) underwent LV myectomy (Morrow procedure), and 3 patients (4%) underwent nonsurgical septal reduction.

At the time of examination, most of the patients (94%) were in sinus rhythm; only few had atrial fibrillation and an implanted pacemaker (1.4% and 4.2%, respectively). ECG findings characteristic of HCM such as Q- and T-wave abnormalities were present in 83% of all cases: 31% of the patients showed abnormal Q waves, while negative T waves were observed in 52% of them.



**Table 3.1.** Clinical features of HCM patients screened in the present study

Number of patients (n)	71	
Age, years	53.3±14.7	
Sex, % (n)		
Male	48.0	(34)
Female	52.0	(37)
Age at diagnosis, years	45.5±16.6	
NYHA class, % (n)		
I	46.5	(33)
II	42.3	(30)
III	9.9	(7)
IV	1.4	(1)
IVS thickness, mm	19.6±3.7	
PW thickness, mm	10.5±2.4	
IVS/PW	1.9±0.5	
LVEDD, mm	45.7±6.0	
Maron type, % (n)		
I	12.7	(9)
II	36.6	(26)
III	45.1	(32)
IV	5.6	(4)
LVOT gradient increased, % (n)	57.7	(41)
SAM, % (n)	53.5	(38)
Morrow myectomy, % (n)	7	(5)
Nonsurgical septal reduction, % (n)	4.2	(3)
Rhythm, % (n)		
Sinus	94.4	(67)
Atrial fibrillation	1.4	(1)
Pacemaker	4.2	(3)
Abnormal Q waves, % (n)	31.1	(22)
Negative T waves, % (n)	52.1	(37)

Data are expressed as mean±standard deviation or as relative (%) and absolute (n) values. Abbreviations used in the table: NYHA, New York Heart Association class of heart failure; IVS, interventricular septum; PW, left ventricular posterior wall; LVEDD, left ventricular end-diastolic dimension; LVOT, left ventricular outflow tract; SAM, systolic anterior motion of mitral valve.

### 3.2 Genetic variants in human *MYL2* and *MYL3*

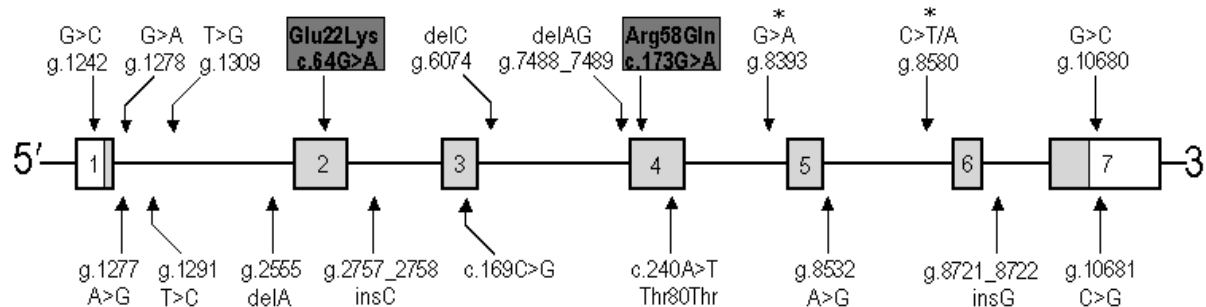
Numbering of identified genetic variants was performed as suggested by Dunnen *et al.*<sup>65</sup> The nucleotide number is preceded by “g.” when a genomic or by “c” when a cDNA reference sequence was used. In *MYL3*, only the cDNA reference sequence was used, because no full-length genomic DNA reference sequence was available. The variants, except those in *MYL3* intronic regions, were simply designated by the nucleotide numbers of the respective reference sequences. For instance, g.8353G>A denotes the G-to-A substitution at nucleotide 8353 of the *MYL2* genomic reference sequence. The *MYL3* intronic variants were designated by the number of nucleotides counted from the first or last nucleotide of an adjacent exon. The negative and positive numbers denote the variant’s location upstream and downstream of an exon, respectively. For instance, c.158-4\_5insGTC denotes an insertion of GTC between nucleotides -4 and -5 upstream of nucleotide 158, which is the first nucleotide of exon 3 according to the *MYL3* reference cDNA sequence.

As it has been already noted in the Material and Methods chapter, the reference sequences used in the present work were obtained from GenBank ([www.ncbi.nlm.nih.gov](http://www.ncbi.nlm.nih.gov)). Accession numbers of these reference sequences are listed in table 3.2. In the present study, self-generated sequences of HCM patients or controls consistent with the reference genomic sequences were designated as wild type sequences.

**Table 3.2.** GenBank accession numbers of the reference sequences used in the present study

	genomic DNA reference sequence	cDNA reference sequence
<i>MYL2</i>	L01652	X66141
<i>MYL3</i>	J04462	M24122

### A) *MYL2*, the ventricular myosin regulatory light chain gene



### B) *MYL3*, the ventricular myosin essential light chain gene

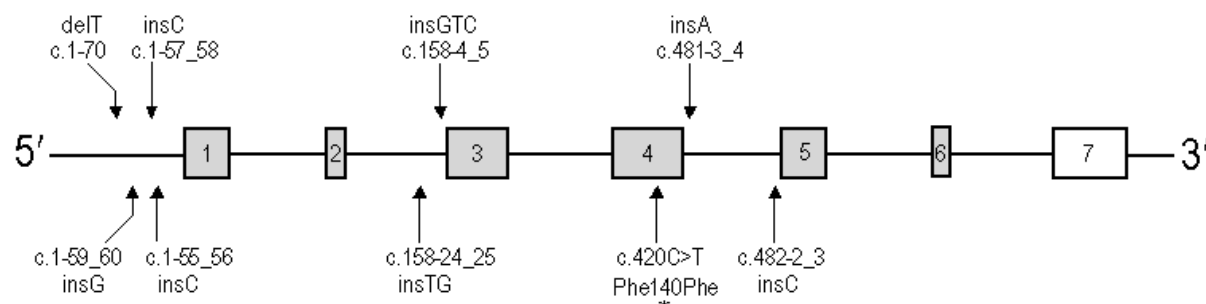


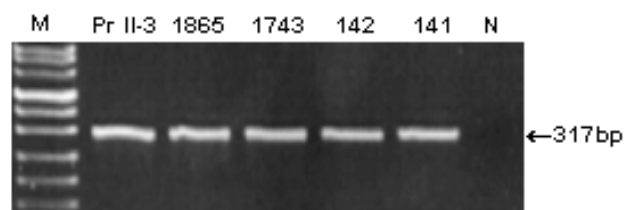
**Figure 3.1. Schematic representation of the ventricular myosin regulatory light chain gene (*MYL2*) and the ventricular myosin essential light chain gene (*MYL3*).** Boxes represent exons, light shaded boxes represent coding DNA of the gene; mutations found in this study are dark shaded; variants with asterisk indicate single nucleotide polymorphisms and the silent mutation; variants without asterisk indicate differences from the reference genomic DNA sequence. Numbering of the genetic variants was performed according to ref. 65. **A)** Location of two missense mutations, SNPs, and sequence differences in *MYL2*. **B)** Location of a silent mutation and sequence differences in *MYL3*.

Two missense mutations, **Glu22Lys** and **Arg58Gln**, were identified in *MYL2* and associated with different HCM phenotypes in two families. The Glu22Lys mutation was identified in exon 2, whereas the Arg58Gln mutation was in exon 4. Additionally, one silent mutation and three single nucleotide polymorphisms (SNPs) were detected while screening the *MYL2* and *MYL3* genes. The **c.420C>T (Phe140Phe)** silent mutation was identified in exon 4 of *MYL3*. The **g.8393G>A** and **g.8580C>T/A** single nucleotide polymorphisms were observed in introns flanking exons 5 and 6 of *MYL2*. Finally, a number of sequence differences from the reference genomic DNA sequence were observed in both genes, most of them in intronic regions. An overview of these findings is given in figure 3.1.

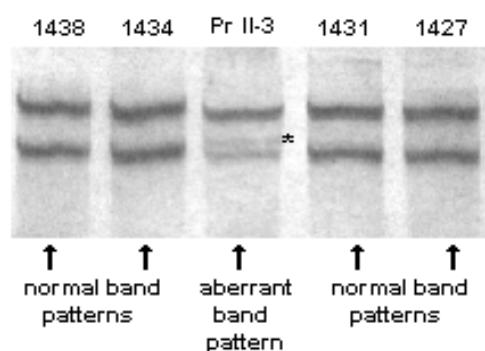
### 3.2.1 Identification of the Glu22Lys mutation in family K

The Glu22Lys mutation was detected initially in patient 1853 (or proband II-3 of family K) during screening of exon 2 of *MYL2*. The sample revealed an aberrant band pattern on SSCP analysis. As shown in figure 3.2 B, the aberrant pattern had three bands instead of two bands as in a normal pattern. Direct automated sequencing of both genomic DNA strands revealed a heterozygous G-to-A (guanine-to-adenine) substitution at nucleotide c.64. On the sequence electropherogram, this was present as two overlapping peaks with a black peak corresponding to G on one allele and a green peak corresponding to A on the other allele (figure 3.2 C). The two overlapping peaks were half the height in comparison with neighbouring peaks and were recognized as "N" by the sequencing analysis software. According to the reference cDNA sequence, this c.64G>A substitution affected the first nucleotide of codon 22 changing it from original **GAA** to mutated **AAA**. This subsequently caused a replacement of glutamic acid (Glu) by lysine (Lys) (**Glu22lys**). In addition to sequencing, the presence of the Glu22Lys mutation was confirmed by RFLP analysis with the *Taq<sup>α</sup>* I restriction enzyme (see further).

## A) PCR

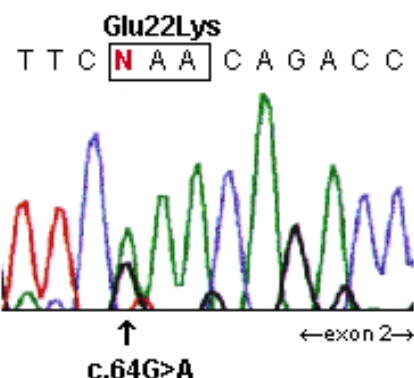


## B) SSCP



## C) Sequencing

## Proband II-3 of family K



## Wild type sequence

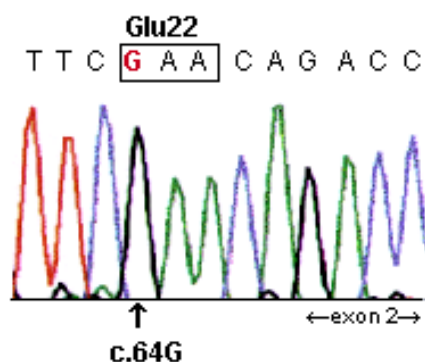


**Figure 3.2. PCR, SSCP analysis and sequencing of exon 2 of *MYL2*.** **A)** A 4% agarose gel loaded with 317-bp PCR products of exon 2. M, VIII-DNA ladder; Pr II-3, proband II-3 of family K; 1865 and 1743, other HCM patients; 141 and 142, control individuals; N, negative control. **B)** Partial SSCP gel. SSCP analysis of proband II-3 of family K (Pr II-3) revealed an aberrant band pattern, which has one additional band (indicated by asterisks) in comparison with patterns shown by neighbouring HCM samples (1438, 1434, 1431, and 1427). **C)** Partial sequence electropherograms of exon 2 of the proband of family K and an individual with the wild type sequence. The proband's electropherogram showed two typical overlapping peaks at nucleotide c.64: a black peak for guanine on the non-mutated allele and a green peak for adenine on the mutated allele. This G-to-A substitution caused a change of glutamic acid to lysine at codon 22. By contrast, the wild type sequence is homozygous for guanine at position c.64.

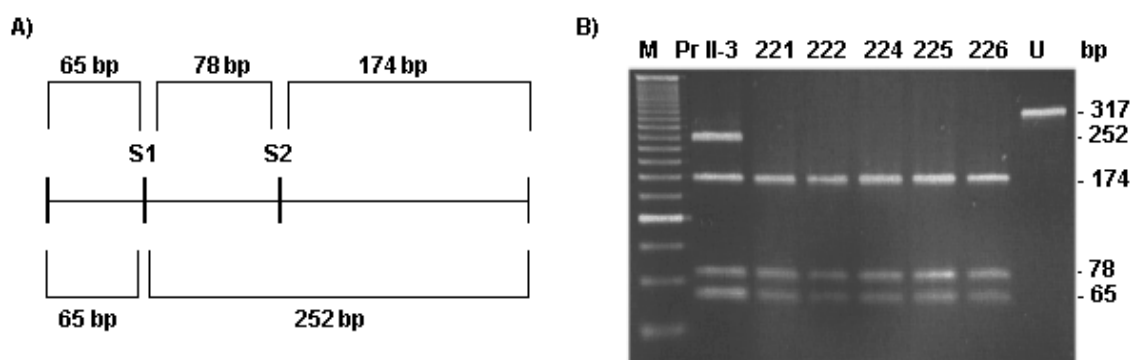


**Figure 3.3. RFLP analysis of exon 2 of *MYL2*.** **A)** Schematic representation of restriction sites of *Taq*<sup>α</sup> I. Two normal S1 and S2 restriction sites produce DNA fragments of 174, 78, and 65 bp. The Glu22Lys mutation removes the S2 restriction site resulting in an abnormal fragment of 252 bp. **B)** The picture of a 4% agarose gel loaded with restriction fragments of the proband of family K (Pr II-3) and controls (221, 222, 224, 225, and 226). The abnormal digestion fragment of 252 bp due to the Glu22Lys mutation is present in the proband of family K but absent in controls. Lane M contains 125-bp DNA ladder. bp, base pairs; U, undigested PCR product of exon 2.

RFLP analysis of proband II-3 and his family members was possible, because the Glu22Lys mutation changed the normal restriction pattern of the *Taq*<sup>α</sup> I restriction enzyme. The wild type sequence of exon 2 possess two normal *Taq*<sup>α</sup> I restriction sites, which produce three DNA fragments of 174, 78, and 65 bp each (figure 3.3 A). *Taq*<sup>α</sup> I recognizes the **TCGA** sequence. The c.64G>A substitution changes this recognition sequence to the **TCAA** sequence and, consequently, removes one of the two normal *Taq*<sup>α</sup> I restriction sites. This will result in the appearance of only two restriction fragments of 65 and 252 bp instead of the three normal fragments (figure 3.3 A). However, the two fragments will be present only when the Glu22Lys mutation is homozygous. In the case of the heterozygous Glu22Lys mutation (as in Family K), the three normal fragments from the non-mutated allele (65, 78 and 174 bp) and the two fragments from the mutated allele (65 and 252 bp) will be observed. On a gel the 65-bp fragments from both alleles will be overlapping each other. Thus, the presence of the Glu22Lys mutation will be recognized by the presence of the additional 252-bp fragment.

Exon 2 of *MYL2* was also amplified from the genomic DNA of control individuals and digested with *Taq*<sup>α</sup> I. 105 controls failed to show the Glu22Lys mutation, because the abnormal 252-bp digestion fragment was observed in none of them (figure 3.3 B).

In the family of patient 1853 (designated as family K; figure 3.4), the Glu22Lys mutation was identified in further six individuals by RFLP analysis: the abnormal restriction fragment of 252 bp was observed in family members II-5, III-2, III-3, III-5, IV-1, and IV-2. In addition to proband II-3, three of these individuals (III-5, IV-1, IV-2) had HCM at the time of examination. The pedigree of family K and results of RFPL analysis are presented in figure 3.4. As shown, the pedigree consisted of 12 individuals over 3 generations. Four individuals (I-1, I-2, II-1, II-2) died before this study, and no data on them could be obtained.

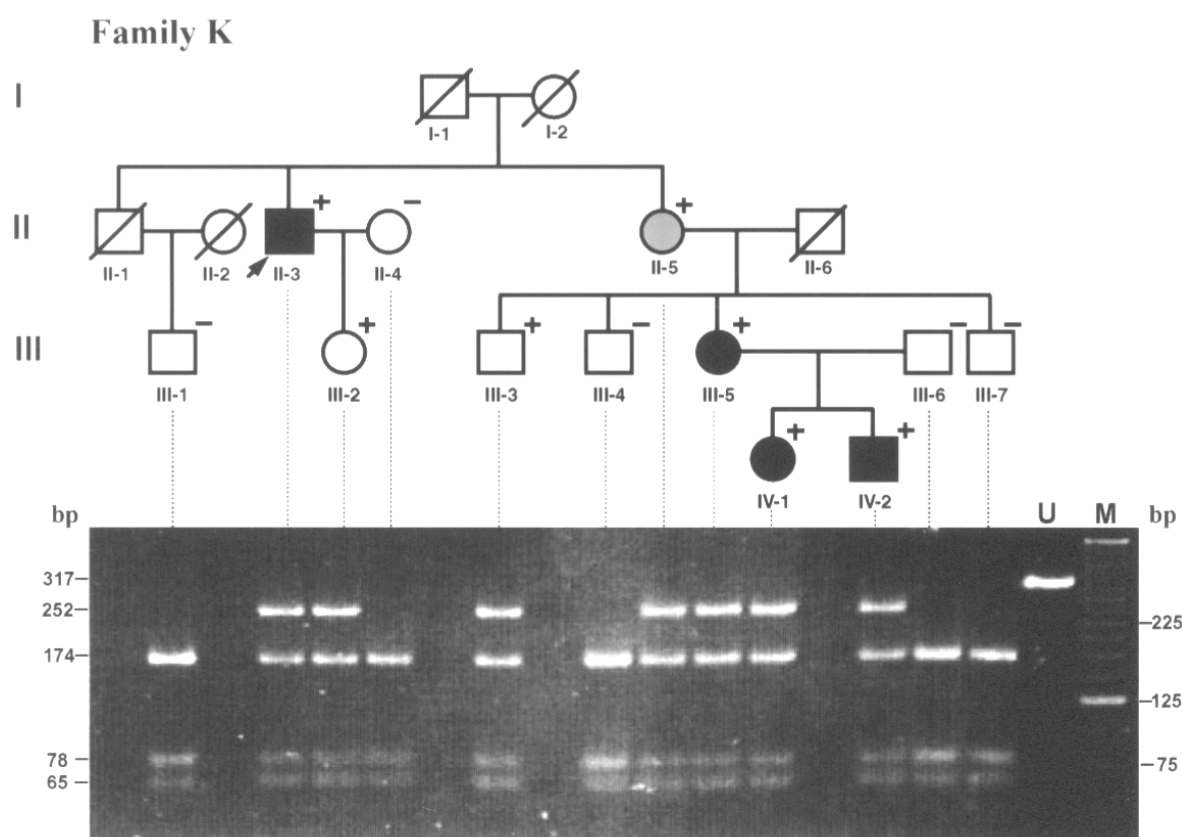
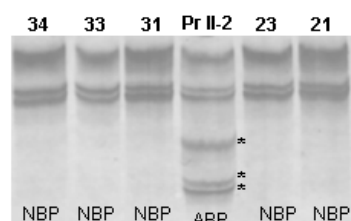


**Figure 3.4. Pedigree of family K and results of RFLP analysis on available family members. Upper panel: Pedigree.** Black symbols represent clinically affected patients; white symbols, clinically unaffected individuals; grey symbol, individuals with uncertain phenotype; symbols with plus sign above, genetically affected individuals; symbols with minus sign above, genetically unaffected individuals; and symbols with diagonal slash, deceased individuals. Proband II-3 (patient 1853) is indicated by arrow. Squares, males; circles, females. **Lower panel: Identification of the Glu22Lys mutation in family members by RFLP analysis with *Taq*<sup>α</sup> I.** A picture of a 4% agarose gel loaded with restriction digests. The abnormal 252-bp fragment is present in family members II-3, III-2, III-3, II-5, III-5, IV-1, and IV-2 indicating the presence of the Glu22Lys mutation. Lane U contains undigested amplification product of *MYL2* exon 2 of 317 base pairs (bp). Lane M contains 125-bp DNA ladder with sizes of bands shown on the right side of the gel picture. Sizes of the digestion products are shown on the left side of the gel picture.

### 3.2.2 Identification of the Arg58Gln mutation in family B

The Arg58Gln mutation was initially identified in patient 1555 (or proband II-2 of family B) while screening exon 4 of *MYL2*. The sample showed an aberrant band pattern (with three clear additional bands) on SSCP analysis (figure 3.5 A). Direct automated sequencing of both DNA strands revealed two typical overlapping peaks indicating a heterozygous G-to-A (guanine-to-adenine) substitution at nucleotide c.173 (figure 3.5 B). The c.173G>A substitution resulted in a replacement of arginine (Arg) by glutamine (Gln) at codon 58 (**Arg58Gln**), because this codon was changed from original **CGA** to mutated **CAA**. The Arg58Gln mutation was confirmed by sequencing in two independent runs, because it did not affect any restriction site making RFLP analysis impossible.

#### A) SSCP analysis



#### B) Sequencing

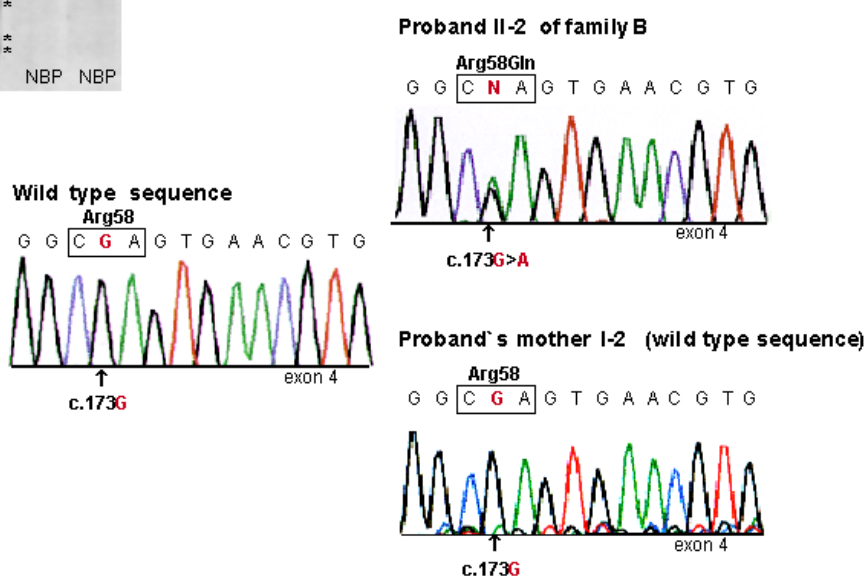


**Figure 3.5. SSCP analysis and sequencing of exon 2 of *MYL2*.** **A)** SSCP analysis. The aberrant band pattern observed in proband II-2 of family B (Pr II-2) was absent in controls (34, 33, 31, 23, and 21) and contains three clear additional bands, which are indicated by asterisks. NBP, normal band pattern; ABP, aberrant band pattern. **B)** Sequence electropherograms of proband II-2 of family B, the proband's mother, and a control individual. Proband II-2 has two overlapping peaks at position c.173 with a black peak corresponding to guanine on the non-mutated allele and a green peak for adenine on the mutated allele. A G-to-A heterozygous substitution resulted in a replacement of arginine by glutamine at codon 58. By contrast, the Arg58Gln mutation was absent in a control and the proband's mother.



In the family of patient 1555 (designated as family B; figure 3.6), two more individuals suffered from HCM: proband's father I-1 and sister II-1. However, genetic analysis on them could not be performed, because they died before this study, and no DNA could be obtained. Genotyping of only alive proband's mother I-2 revealed no Arg58Gln mutation (figure 3.5 B and 3.6). The pedigree of family B with results of SSCP analysis on patient 1555 and her mother is presented in figure 3.6.

Exon 4 of *MYL2* was further amplified from DNA of control individuals and subjected to SSCP analysis. 105 controls failed to show the Arg58Gln mutation, because none of them revealed the aberrant band pattern characteristic of this mutation (figure 3.5 A).

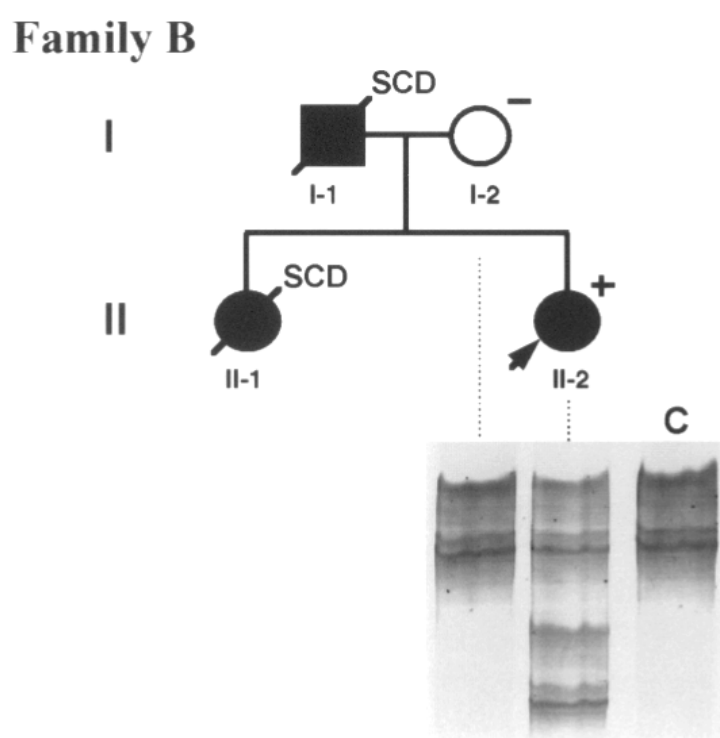


**Figure 3.6. Pedigree of family B and results of SSCP analysis. Upper panel: Pedigree.** Black symbols represent clinically affected patients; white symbols, clinically unaffected individuals; symbols with plus sign above, genetically affected individuals; symbols with minus sign above, genetically unaffected individuals; symbols with diagonal slash, deceased individuals; squares, males; and circles, females. The proband (patient 1555) is indicated by arrow. SCD, sudden cardiac death. **Lower panel: SSCP gel.** Proband II-2 showed an aberrant mobility pattern absent in her mother (I-2) and control (C).

### 3.2.3 Localization of the mutations in highly conserved RLC regions

The amino acid residues affected by the Glu22Lys and Arg58Gln mutations are strictly conserved throughout evolution: as shown in figure 3.7, glutamic acid at position 22 and arginine at position 58 are invariant in RLC isoforms, which are expressed in the heart of different species (human ventricular/slow skeletal, rat and mouse ventricular, chicken cardiac). Glutamic acid is also preserved among skeletal isoforms of the shown species.

The identified Glu22Lys and Arg58Gln mutations are located in the amino terminal half of the RLC, which contains two putatively important functional regions: the phosphorylation and calcium-binding sites. As shown in figure 3.8, both variants are in  $\alpha$ -helices flanking the calcium-binding loop. The Glu22Lys is additionally in the region adjacent to the RLC phosphorylation site.

The Glu22Lys and Arg58Gln mutations are further predicted to alter the normal net charge of the RLC N-terminus, because the Glu22Lys variant caused a replacement of negatively charged glutamic acid by positively charged lysine, and the Arg58Gln mutation caused a substitution of positively charged arginine by non-charged glutamine.

Glu22Lys (E22K) Arg58Gln (R58Q)	K										Q	
	17	22	30	40	50	58	70	77				
<b>RLC</b>												
Human ventricular/slow skeletal	VFSMF	EQTQIQEFKEAFTIMDQNRDGFIDKNDLRDTFAALG				R	VNVKNEE	IDEM I KEAPGPI				
Rat ventricular	VFSMF	EQTQIQEFKEAFTIMDQNRDGFIDKNDLRDTFAALG				R	VNVKNEE	IDEM I KEAPGPI				
Mouse ventricular	VFSMF	EQTQIQEFKEAFTIMDQNRDGFIDKNDLRDTFAALG				R	VNVKNEE	IDEM I KEAPGPI				
Chicken cardiac A	VFSMF	EQAQIQEFKEAFTIMDQNRDGFIDKADLRDTFAALG				R	LVNKNEE	IDEM I KEAPGPI				
Rat skeletal	VFSMF	DQTQIQEFKEAFTVI DQNRDGI IDKEDLRDTFAAMG				R	LVNKNEELDAMMKEASGPI					
Mouse skeletal	VFSMF	DQTQIQEFKEAFTVI DQNRDGI IDKEDLRDTFAAMG				R	LVNKNEELDAMMKEASGPI					
Rabbit skeletal	VFSMF	DQTQIQEFKEAFTVI DQNRDGI IDKEDLRDTFAAMG				R	LVNKNEELDAMMKEASGPI					
Chicken skeletal	VFSMF	DQTQIQEFKEAFTVI DQNRDGI IDKDDLRETFAMG				R	LVNKNEELDAM I KEASGPI					
Human smooth	VFAMF	DQSQIQEFKEAFNMIDQNRDGFIDKEDLHDMLASMG				K	NPTDEYLDAMMNEAPGPI					
Rat smooth	VFAMF	DQSQIQEFKEAFNMIDQNRDGFIDKEDLHDMLAS LG				K	NPTDEYLEGMMSEAPGPI					
Chicken smooth	VFAMF	DQSQIQEFKEAFNMIDQNRDGFIDKEDLHDMLAS LG				K	NPTDEYLEGMMSEAPGPI					
Pig smooth	VFAMF	DQSQIQEFKEAFNMIDQNRDGFIDKEDLHDMLASMG				K	NPTDEYLEGMMSEAPGPI					

**Figure 3.7. Amino acid alignment across species and RLC isoforms.** The Glu22Lys and Arg58Gln mutations affect the highly conserved amino acids, suggesting the essentiality of these residues for normal protein function. RLCs from the same muscle type show the highest sequence homology. This indicates that functional properties of a protein are determined by its amino acid sequence. Glu and E, glutamic acid; Lys and K, lysine; Arg and R, arginine; Gln and Q, glutamine.

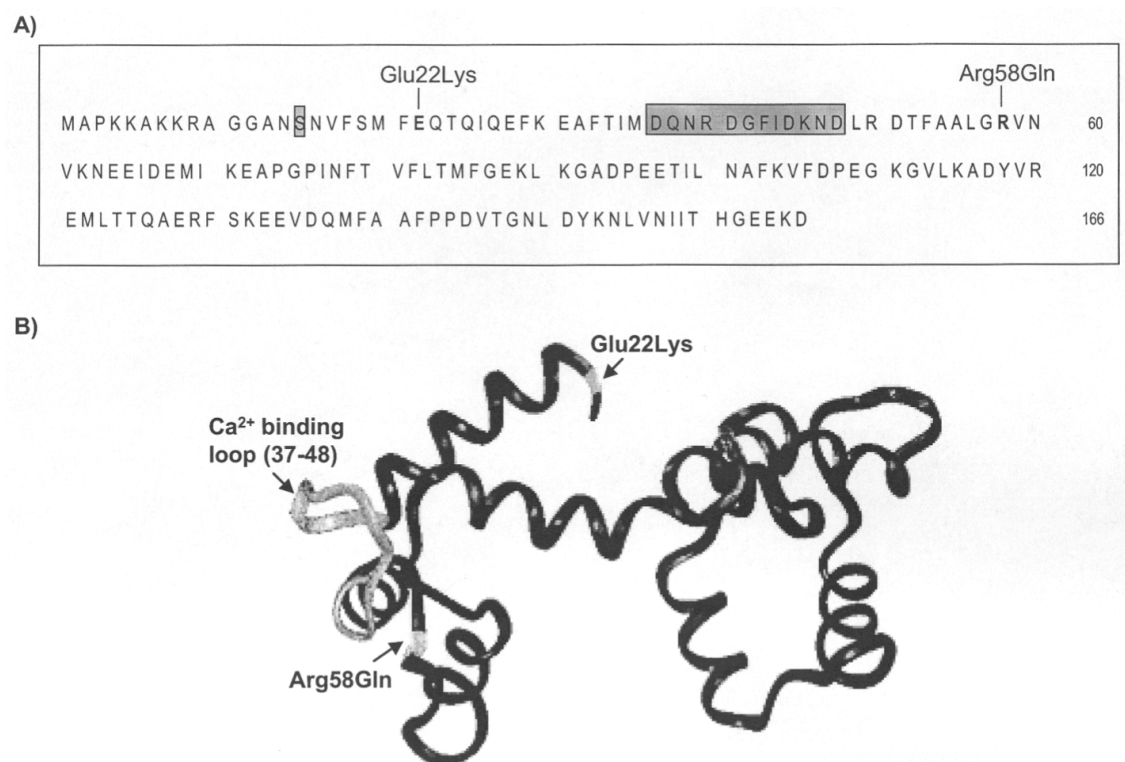


**Figure 3.8. Localization of the Glu22Lys and Arg58Gln mutations in the RLC sequence (A) and three-dimensional structure (B).** The putative phosphorylation site at serine-15 (A) and calcium-binding site at residues 37-48 (A, B) are highlighted. As shown, the Glu22Lys mutation is located close to the RLC phosphorylation site, moreover it is in the  $\alpha$ -helix flanking the calcium-binding loop. The Arg58Gln mutation is in the  $\alpha$ -helix, which flanks the calcium-binding loop from the other side. Adapted from ref. 29.

### 3.2.4 Clinical features of family K with the Glu22Lys mutation

Clinical data of the genetically affected members of families K and B are summarized in table 3.3.

In family K, the Glu22Lys mutation was identified in seven individuals. Within them, four individuals had HCM (II-3, III-5, IV-1, and IV-2), one individual had borderline cardiac hypertrophy (II-5), and another one (III-2) was a healthy carrier. Remaining genetically affected individual III-3 (32 years old) had normal ECG, but echocardiographic evaluation could not be performed because of patient's unwillingness. All these individuals were asymptomatic apart from proband II-3 and his sister II-5.

75-year old male proband II-3 was referred for clinical evaluation because of episodes of palpitation, chest pain, and dyspnea. His ECG showed sinus rhythm and left bundle branch block. Holter electrocardiography demonstrated an episode of supraventricular tachycardia and polytopic ventricular extrasystoles. Echocardiography revealed asymmetric hypertrophy with IVS of 23 mm. No LV cavity or outflow tract obstruction was observed. Within the following year, the proband was admitted to Franz-Volhard-Klinik twice because of events of atrial fibrillation. During the first visit, he was converted to sinus rhythm by electrical cardioversion. The next time, he underwent a successful high frequency ablation.

Genetically affected proband's niece III-5, 42 years old, did not report any symptoms. But her ECG demonstrated abnormal Q waves at leads I and aVL. Echocardiography revealed basal septal hypertrophy of 15 mm. No pressure gradient was present.

20-year old female individual IV-1, who inherited the Glu22Lys mutation from her mother III-5, also did not show any clinical symptoms but had abnormal ECG, and echocardiographic findings characteristic of HCM. Her ECG demonstrated pathologic Q waves at aVL, while echocardiography revealed midseptal hypertrophy related to body surface area with IVS thickness of 12 mm. No LV cavity or outflow tract obstruction was observed.

Similarly, 18 year-old male individual IV-2, who also inherited the mutation from his mother III-5, did not report any clinical symptoms but exhibited ECG and echocardiographic abnormalities characteristic of HCM. ECG showed voltage criteria of

LV hypertrophy: Sokolow-Lyon index was 4.8 mV. Echocardiography demonstrated midseptal hypertrophy of 13 mm without any obstruction.

The phenotype of genetically affected proband's sister II-5 was defined as "uncertain". The 62-year old woman reported periodic dyspnea and chest pain. But her ECG was normal. Echocardiography revealed IVS of 13 mm, however, it was in the normal range in relation to her body surface area of 2.45 m<sup>2</sup>. No pressure gradient was present.

33-year old proband's daughter III-2, who inherited the mutation, reported no clinical symptoms. Her ECG revealed pathologic Q waves at lead aVF, but echocardiography showed no myocardial hypertrophy.

**Table 3.3.** Clinical features of genetically affected individuals of families K and B

Family	Family K						Family B
Pedigree number	II-3	II-5	III-2	III-5	IV-1	IV-2	II-2
Mutation	Glu22Lys	Glu22Lys	Glu22Lys	Glu22Lys	Glu22Lys	Glu22Lys	Arg57Gln
Age (years)	75	62	33	42	20	18	27
Age at diagnosis (years)	75	62	33	42	20	18	7
BSA (sqm)	1.97	2.45	2.08	2.06	1.75	2.01	1.58
Weight (kg)	81	139	98	96	65	80	56
Heart block	LBBB	no	no	no	no	no	no
Negative T	n.a.	no	no	no	no	no	yes
Abnormal Q	n.a.	no	aVF	I, aVL	aVL	no	no
S-L index (mV)	n.a.	1.9	2.4	3.1	2.2	4.8	4.8
<b>IVS (mm)</b>	<b>20</b>	<b>13</b>	<b>10</b>	<b>15</b>	<b>12**</b>	<b>13</b>	<b>21</b>
PW (mm)	13	n.d.	7	8	7	10	7
IVS/PW	1.5	n.a.	1.4	1.8	1.7	1.3	3
LVEDD (mm)	52	47	48	53	44	52	39
Maron type of LVH*	I	I	n.a.	I	IV	IV	III
NYHA class	III	II	I	I	I	I	II
Clinical status	affected	uncertain	unaffected	affected	affected	affected	affected

BSA, body surface area; S-L index, Sokolow-Lyon index; IVS, interventricular septum; PW, left ventricular posterior wall; LVEDD, left ventricular end-diastolic dimension; LBBB, left ventricular bundle branch block; LVH, left ventricular hypertrophy; NYHA, New York Heart Association class of heart failure; n.d., not determined; n.a., not applicable. \*According to ref. 28. \*\*In this individual, HCM diagnosis was based on increased IVS thickness for his age, weight and BSA.

### 3.2.5 Clinical features of family B with the Arg58Gln mutation

In family B, three individuals had HCM, two of them died suddenly at young age.

The proband II-2 was 7 years old when HCM was diagnosed during a medical evaluation because of sudden cardiac death of her 28-year old father. When she was 16 years old, therapy with  $\beta$ -adreno receptor blockers was started due to premature fatigue on exertion. At the age of 25, the patient additionally reported palpitations and presyncopal conditions. She was referred to an electrophysiological examination; during this procedure she developed ventricular tachycardia degenerating into ventricular fibrillation. The proband was converted to sinus rhythm by electrical defibrillation. Afterwards, considering the family history of two sudden cardiac deaths and aggravation of clinical symptoms, a cardioverter-defibrillator (ICD) was implanted. At the age of 27, recurrent events of supraventricular tachycardia (up to 170/min) were registered on the ICD, and she was admitted to Franz-Volhard-Klinik. No shock had been delivered from the ICD by that time. ECG showed voltage signs of LV hypertrophy with T wave inversion. Echocardiography revealed asymmetric septal hypertrophy of 21 mm extending to the LV apex and lateral free wall. No pressure gradient was observed. Electrophysiological investigation demonstrated the common type of atrial flutter with 2:1 conduction ratio. Ablation therapy was considered, but due to the risk of affecting the ICD lead, therapy with sotalol was attempted first. The latter resulted in suppression of the tachycardia and improvement of clinical symptoms.

Proband's mother I-2 did not have HCM: she had a normal ECG and LV wall thickness on echocardiography.

Proband's father I-1 did not show any symptoms of the disease. He died suddenly at the age of 28. It is known from his wife that HCM was diagnosed on autopsy.

Clinical data on proband's younger sister II-1 were kindly sent by Prof. Kienast from the University Clinic in Rostock. She was 5 years old when HCM was diagnosed. The only symptom reported was premature fatigue on exertion. Her ECG showed signs of LV hypertrophy with negative T waves in left chest leads. Echocardiography demonstrated septal hypertrophy of 26 mm, normal thickness of LV posterior wall, and LV outflow tract obstruction. Despite regular medical check-ups and treatment by calcium channel blockers, she died suddenly at home at the age of 21.

### 3.2.6 The c.420C>T (Phe140Phe) silent mutation in *MYL3*

In *MYL3*, the c.420C>T (**Phe140Phe**) silent mutation was detected in one patient (DNA sample 1635) out of the 71 individuals while screening exon 4. The sample showed an aberrant band pattern on a SSCP gel. As shown in figure 3.9 B, the aberrant band pattern possessed an additional band in comparison with normal patterns shown by the neighbouring samples. DNA sequencing revealed a heterozygous C-to-T (cytosine-to-thymine) substitution at nucleotide c.420 (figure 3.9 C). No amino acid change was caused by this substitution, because both codons **TTC** and **TTT** encode for phenylalanine.

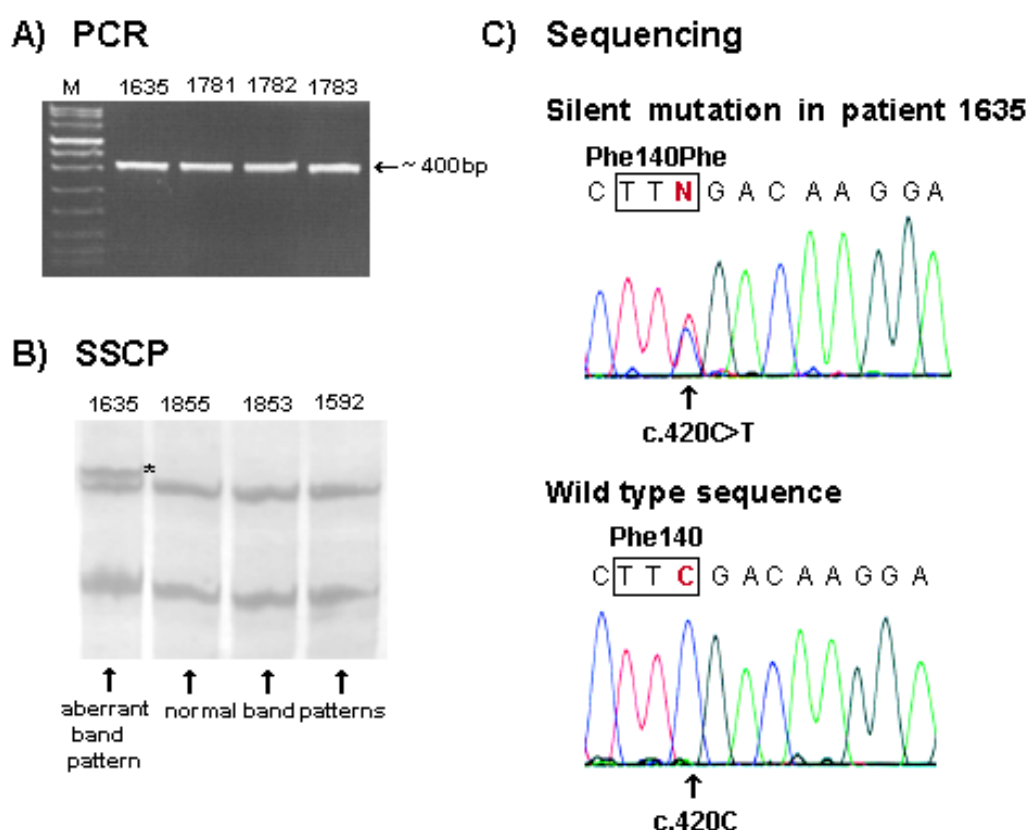


**Figure 3.9. PCR, SSCP analysis and sequencing of exon 4 of *MYL3*.** **A)** A 4% agarose gel loaded with PCR products of exon 4. The amplified fragments were approximately 400 base pairs (bp) long. Lane M contains VIII-DNA ladder. 1635, a patient carrying the c.420C>T polymorphism; 1781, 1782, and 1783, other HCM patients. **B)** SSCP analysis of patient 1635 revealed an aberrant band pattern, which has an additional band (indicated by asterisk) in comparison with patterns shown by neighbouring HCM patients 1855, 1853, and 1592. **C)** Partial sequence of patient 1635 showing the heterozygous c.420C>T silent mutation and of an individual homozygous for the wild type *MYL3* allele.

### 3.2.7 Single nucleotide polymorphisms in *MYL2*

SSCP analysis of PCR products containing exons 5 and 6 and their flanking intronic regions revealed different band patterns, which were unevenly distributed but frequent. This suggested that eventually some common genetic variants underlie the observed SSCP band patterns. Although the relatively high frequency of each band pattern within a group of 71 patients suggested that underlying genetic variants are not disease-causing mutations but rather polymorphisms, in order not to miss any disease-causing mutation, several samples from each subset of samples showing a similar SSCP pattern were selected for sequencing. The latter revealed the **g.8393G>A** and **g.8580C>T/A** intronic single nucleotide polymorphisms confirming the initial proposal about common polymorphisms.



### ***The g.8393G>A polymorphism in intron 4 of MYL2***

After evaluating SSCP gels of the exon 5 fragment, seven samples were sequenced. Two *MYL2* allelic variants were observed with regard to nucleotide position g.8393 in the part of intron 4 flanking exon 5. The first one was a **g.8393G** variant, which designates the presence of guanine at nucleotide position g.8393. This variant corresponded to the reference genomic DNA sequence and was therefore considered the wild type sequence. The second variant was **g.8393G>A**, which denotes a *MYL2* allele possessing adenine at the same g.8393 nucleotide position.

Within the seven sequenced samples, three samples (1595, 1808, and 1744) were homozygous for the g.8393G wild type allele (figure 3.10 A). Three further individuals (1795, 1811, and 1817) were heterozygous for the g.8393G and g.8393G>A alleles (figure 3.10 C). The remaining sample (1819) was homozygous for the g.8393G>A polymorphism (figure 3.10 B).

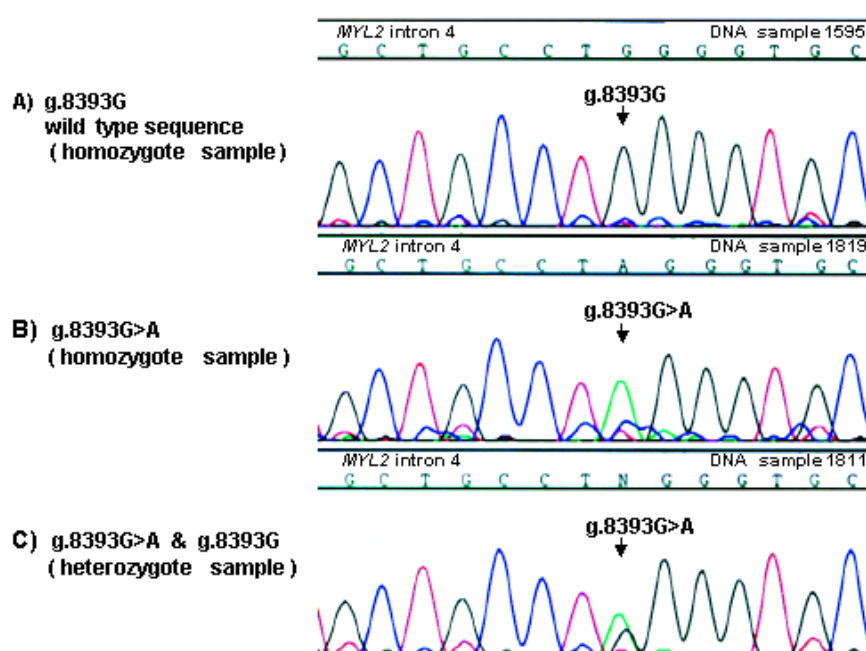


**Figure 3.10. Partial sequence electropherograms of intron 4 of *MYL2* showing genetic variants at position g.8393. A)** DNA sequence of sample 1595 with guanine at nucleotide position g.8393 on both alleles. **B)** DNA sequence of patient 1819 showing the presence of the homozygous g.8393G>A polymorphism. **C)** DNA sequence of patient 1811 showing the presence of the heterozygous g.8393G>A polymorphism.

### ***The g.8580C>T/A polymorphism in intron 5 of MYL2***

In the case of the *MYL2* exon 6 fragment, eight samples underwent DNA sequencing, which revealed three allelic variants with regard to nucleotide position g.8580 in the part of intron 5 flanking exon 6. The first variant was **g.8580C**, which denotes an allele with cytosine at nucleotide position g.8580. This variant was consistent with the reference genomic DNA sequence and was considered the wild type sequence. The second identified variant was **g.8580C>T**, which designates a *MYL2* allele carrying thymine at nucleotide g.8580. The third variant was **g.8580C>A**, which denotes an allele possessing adenine at the same g.8580 position.

Among eight sequenced samples, two samples (1584, 1781) were homozygous for the g.8580C wild type allele (figure 3.11 B). Three further samples (1565, 1744, and 1782) were heterozygous for the g.8580C and g.8580C>T alleles (figure 3.11 D). Two other individuals (1707 and 1780) were homozygous for the g.8580C>T polymorphism (figure 3.11 A). The remaining sample (1594) was heterozygous for the g.8580C>T and g.8580C>A alleles (figure 3.11 C).

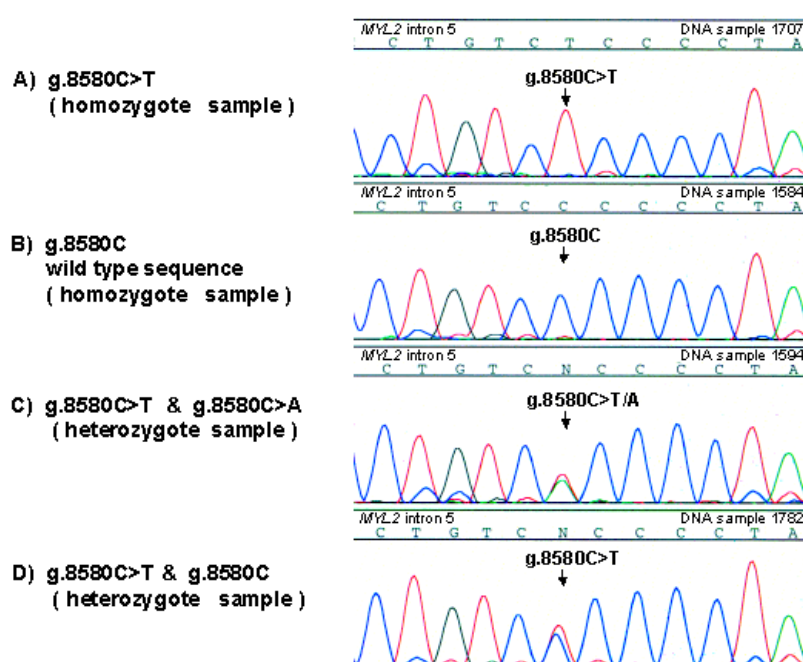


**Figure 3.11. Partial sequence electropherograms of intron 5 of *MYL2* showing genetic variants at position g.8580. A)** DNA sequence of patient 1707 showing the homozygous g.8580C>T polymorphism. **B)** DNA sequence of wild type sample 1584 with guanine at position g.8580 on both alleles. **C)** DNA sequence of patient 1594 showing the presence of the g.8580C>T polymorphism on one allele and the g.8580C>A polymorphism on the other allele. **D)** DNA sequence of patient 1782 showing the presence of the heterozygous g.8580C>T polymorphism.

Both g.8393G>A and g.8580C>T/A *MYL2* variants were located in intronic regions and did not cause an amino acid exchange. Furthermore, these polymorphisms are not predicted to have any effect on the splicing process proceeding from their localizations sufficiently far from the splice sites.

After clarifying that no disease-causing mutations but nucleotide polymorphisms did underlie the observed SSCP band patterns, no further sequencing of the exon 5 and exon 6 containing fragments was performed.

### 3.2.8 Genomic sequence differences

While evaluating data obtained in the course of this study, some self-generated genomic DNA sequences had regions (further designated as differences), which mismatched to the reference genomic DNA sequences. These nucleotide differences were considered such rather than polymorphisms or mutations, because they were present in *all samples* subjected to DNA sequencing. Proceeding from the high quality of self-generated sequences, it was concluded that the observed differences were due to the errors in the reference genomic DNA sequences. This conclusion was confirmed by further analysis of the self-generated sequences in comparison to the reference cDNA sequences. The presence of eventual errors in the reference genomic DNA sequences required careful analysis in order to interpret obtained data accurately.

All observed differences were in intronic regions of both genes, except for **c.240A>T** and **c.169C>G** differences, which were detected in the coding part of *MYL2* (see overview in figure 3.1). As indicated in figure 3.1, the differences were present as nucleotide substitutions (n=10), nucleotide deletions (n=4) and insertions (n=9).

Figure 3.12 below shows examples of the observed differences in intron 1 (**g.1277A>G**, **g.1278G>A** and **g.1291T>C**) and in exon 4 (**c.240A>T**) of *MYL2*. As shown, the c.240A>T difference was observed in comparison to the reference genomic DNA sequence but was in agreement with the reference cDNA sequence.

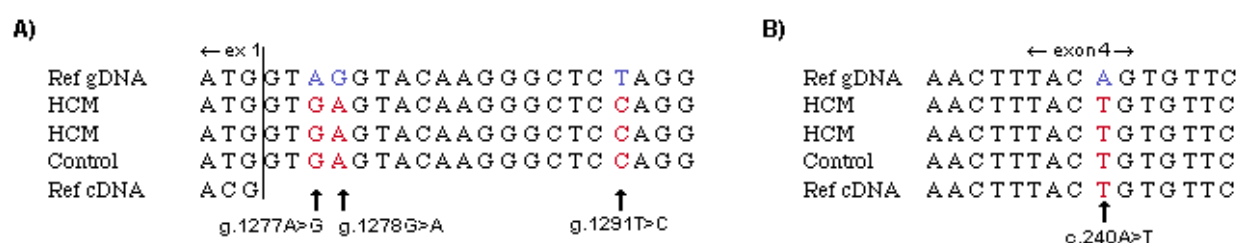


**Figure 3.12. Partial sequence alignment of HCM samples, control and the reference genomic DNA and cDNA sequences.** Ref gDNA, the reference genomic DNA sequence; HCM, self-generated DNA sequence of a HCM patient; control, self-generated DNA sequence of a control individual; cDNA, the reference cDNA sequence. **A)** Partial sequence alignment of intron 1 of *MYL2*. Three identified differences, g.1277A>G, g.1278G>A and g.1291T>C, are highlighted. **B)** Partial sequence alignment of exon 4 of *MYL2* with the c.240A>T difference highlighted.

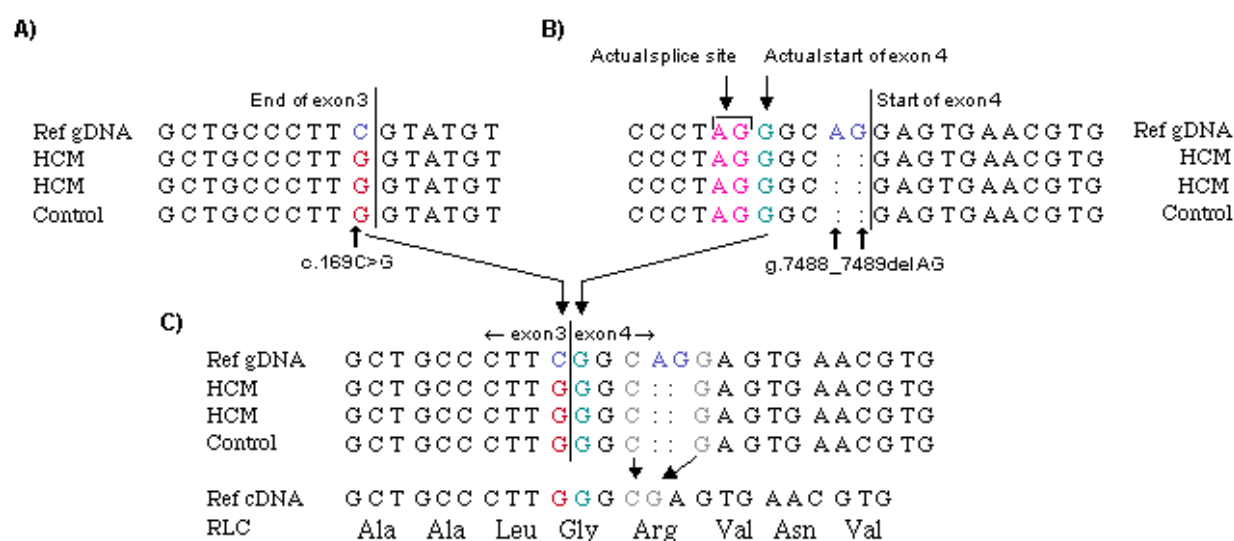


**Figure 3.13. Partial sequence alignment of HCM samples, control and the reference genomic DNA and cDNA.** Ref gDNA, the reference genomic DNA sequence; HCM, self-generated DNA sequence of a HCM patient; control, self-generated DNA sequence of a control individual; cDNA, the reference cDNA sequence; RLC, RLC amino acid sequence translated on the basis of the reference cDNA sequence. **A)** Sequence alignment of exon 3 and a donor splice site of intron 3 of *MYL2*. The c.169C>G difference is highlighted. **B)** Sequence alignment of exon 4 of *MYL2*. The deletion of adenine and guanine (g.7488\_7489delAG) at the acceptor splice site of exon 4 is highlighted. The actual splice site is shown three nucleotides upstream. **C)** Exon 3 and 4 of *MYL2* are aligned together to show that the self-generated sequences are in agreement with the reference cDNA but not with the genomic DNA sequences.

The most confusing findings were the **c.169C>G** and **g.7488\_7489delAG** differences identified in *MYL2*. The c.169C>G difference denotes the presence of guanine instead of cytosine at nucleotide c.169, which is the last nucleotide of exon 3 (figure 3.13 A). The **g.7488\_7489delAG** difference denotes a deletion of the AG acceptor splice site of exon 4 (figure 3.13 B). But another AG splice site was found three nucleotides upstream and is predicted to be the actual acceptor splice site of exon 4 proceeding from the comparison with the c.DNA reference sequence.

The presence of the **c.169C>G** difference and shift of the acceptor splice site of exon 4 upstream resulted in three more nucleotides **GGC** at the beginning of exon 4. This subsequently resulted in two rearranged codons: **GGG** encoding for glycine and **GCA** encoding for arginine. These findings were in agreement with the reference cDNA sequence as shown in figure 3.13 C.

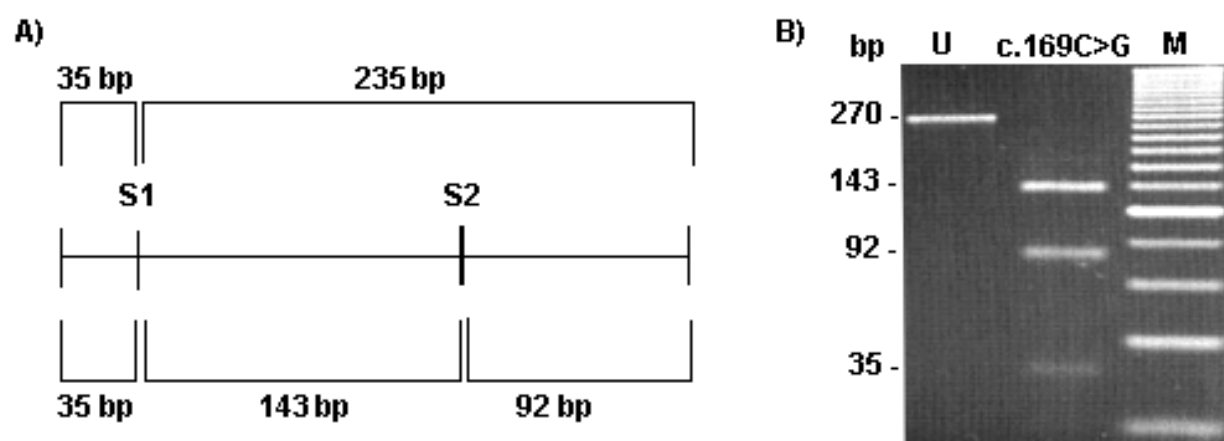


**Figure 3.14. RFLP analysis of exon 3 of *MYL2*, which confirmed the presence of the c.169C>G difference in all of 71 HCM-patients and 100 control individuals. A)** Schematic drawing of the restriction sites of *Sty* I. According to the *MYL2* genomic DNA reference sequence, an amplified product of exon 3 is supposed to have only one restriction site (S1), which gives rise to two digests of 35 and 235 base pairs (bp) each. But in the presence of the c.169C>G difference, it has two restriction sites (S1 and S2), which produce three restriction fragments of 35 bp, 92 bp, and 143 bp each. **B)** A picture of 4% agarose gel loaded with digests. The presence of three restriction fragments of 35, 92, and 143 bp but not two of 35 and 235 confirms the presence of the c.169C>G difference and of an error in the genomic DNA reference sequence. The same band pattern as shown on this gel was observed in all 71 patients and 100 controls. Lane U contains undigested amplification product of exon 3 of 270 base pairs. Lane M contains 125-bp DNA ladder.

In the case of the c.169C>G difference, it was possible to perform RFLP analysis with the *Sty* I restriction enzyme. This enzyme recognizes the sequence **CCTTGG**. According to the *MYL2* genomic reference sequence, the amplified fragment containing exon 3 (270 bp long) is supposed to possess a single *Sty* I restriction site, which produces two DNA fragments of 35 and 235 bp each (figure 3.14). However, the c.169C>G difference introduces an additional *Sty* I recognition site. Collectively, the two *Sty* I restriction sites will result in three fragments of 35, 143, and 92 bp. The observation of these three fragments in all 71 HCM probands and 100 controls confirmed the presence of an error in the reference genomic DNA sequence at nucleotide c.169 (figure 3.14).

## 4 Discussion

The ventricular myosin essential (*MYL3*) and regulatory light chain (*MYL2*) genes were analysed in a group of 71 unrelated clinically well-characterized HCM patients. Systematic analysis revealed two missense mutations in *MYL2* associated with either benign or malignant HCM phenotype. Additionally, one silent mutation, two single nucleotide polymorphisms (SNPs), and a number of sequence differences were detected while screening the *MYL2* and *MYL3* genes.

### 4.1 Patient cohort and screening approach

The patients enrolled in the present study revealed typical features of HCM and were well representative of the overall HCM population.<sup>56</sup> Similarly to other studies, the age of the patients varied widely, however, most of them were already at midlife at the time of diagnosis.<sup>5,44,66</sup> The majority of the patients had mild or no symptoms and were diagnosed after the third decade of their life. In most cases, LV hypertrophy involved the entire IVS or both IVS and the free wall. These two patterns of hypertrophy distribution have also been previously described as the most common in HCM.<sup>45</sup> Despite the high number of patients with obstructive HCM in the present cohort, operative management of obstruction was performed only in few of them. This suggests that the number of patients with massively increased pressure gradient and in the need of operative treatment in the overall population of HCM patients is small in comparison with the number of individuals, who can be treated by drugs.

Among a variety of available techniques,<sup>67</sup> the PCR-SSCP method used in the present work has been shown to be a reliable and informative method for detecting unknown mutations in DNA fragments of interest.<sup>64,67,68</sup> Although it has been argued

that the 80-90% sensitivity of SSCP analysis does not exclude a possibility of some mutations remaining undetected, there is a common agreement that this method is the most suitable for mutation screening in a large patient group, because it is economical, rapid and simple in carrying out. Moreover, the sensitivity of SSCP analysis can be significantly increased by adjusting the running conditions.<sup>63,69</sup> In the present work, two SSCP runs under different conditions were used to screen each of coding exons in order to achieve a high detection rate and to decrease the number of missed genetic variants. Furthermore, since the SSCP analysis is more sensitive for shorter DNA fragments,<sup>64</sup> most of the PCR fragments were 150-400 base pairs in length. The efficiency of SSCP analysis in the present study is supported by the identification of such minor DNA changes as SNPs and point mutations. Notably, results of SSCP analysis were always consistent with the results of DNA sequencing: each of the observed aberrant SSCP patterns had an underlying sequence variation. By contrast, sequence differences did not show any aberrancy on SSCP. Observation of high number of sequence differences also underlines the possibility of frequent errors in reference sequences, and how careful one should be in using them.

It is necessary to note that the present work did not aim to study genetic polymorphisms but disease-causing mutations. SNPs were determined in the course of this study, because they mimic disease-causing mutations on the SSCP analysis. SNPs are common single nucleotide allelic variations, which are present at least in 1% of a population.<sup>70</sup> According to recent studies, SNPs occur on average every 1,000-2,000 nucleotides.<sup>70-72</sup> It is supposed that they account for much of the functional heterogeneity in gene expression and protein activity exhibited in the human population.<sup>72,73</sup> In contrast to disease mutations, SNPs do not directly cause any disorder, however, recent studies showed that SNPs or particular combinations of them might be associated with individual susceptibility to common polygenic disorders (diabetes, cancer, cardiovascular and neurological diseases, and others).<sup>57,71,74,75</sup>

In the present study, the exact distribution of the observed SNPs among the 71 examined patients was not estimated, because, firstly, it was not consistent with the study purposes, and, secondly, it would have required sequencing of corresponding DNA fragments in all patients. However, recurrent observation of the SSCP patterns characteristic of g.8393 G>A and g.8580 C>T/A indicates that these polymorphisms are common sequence variations. According to SSCP analysis, the frequency of these



variants in this study population was much more than 1%. Interestingly, the g.8393G>A polymorphism was also observed in South African as well as Danish HCM patients and controls.<sup>16</sup> Thus, further studies are needed to determine the frequency of the *MYL2* g.8393G>A and g.8580C>T/A polymorphisms and whether they have any implication in HCM or other diseases.

## 4.2 The Glu22Lys and Arg58Gln mutations in *MYL2*

HCM is caused by mutations in nine genes encoding for sarcomeric proteins including those for ventricular myosin light chains, although the frequency of mutations in each of these genes is variable.<sup>3</sup> In the present study, screening of 71 unrelated HCM patients revealed only two mutations in *MYL2* and no mutation in *MYL3*. These data underline the rarity of ELC/RLC mutations in HCM. The absence of mutations in *MYL3* confirms that the contribution of ELC mutations to the HCM causes is significantly less than that of RLC mutations.<sup>15,16</sup> In a study, which was previously conducted in our lab, an independent group of 85 HCM patients was screened, and neither *MYL2* nor *MYL3* mutations were found (unpublished data). Collectively, 186 unrelated HCM patients (71 patients from the present study and 85 from the previous study) underwent genetic analysis in two independent studies in our lab: the frequency of *MYL2* mutations in this relatively large patient cohort is approximately 1%. These data are consistent with data obtained by Potter *et al.*<sup>10</sup> but not with data from later studies, which estimated the frequency of *MYL2* mutations as 4.4%<sup>15</sup> and 7%.<sup>16</sup>

So far, only three disease-associated mutations have been identified in the ELC gene.<sup>10,59</sup> In the RLC gene, seven point and one splice site mutations have been detected.<sup>10,15,16</sup> These mutations and available information on associated phenotypes are listed in table 4.1. In contrast to some other genes, limited number of families confounds generally applicable conclusions regarding the disease course and prognosis in HCM caused by myosin light chain gene mutations. Therefore, in rare HCM forms, every single family, identified, becomes valuable.

**Table 4.1.** The known HCM associated mutations in the RLC and ELC genes

Gene	Exon	Mutation	Number of families	Associated phenotype	Reference
MYL2	2	Ala13Thr	1 individual	midventricular hypertrophy	Poetter <i>et al</i> , 1996 <sup>10</sup>
	2	Ala13Thr	1 family	septal hypertrophy, good prognosis and survival	Andersen <i>et al</i> , 2001 <sup>16</sup>
	2	Phe18Leu	1 family	septal hypertrophy	Flavigny <i>et al</i> , 1998 <sup>15</sup>
	2	<b>Glu22Lys</b>	2 brothers and 1 unrelated individual	midventricular hypertrophy	Poetter <i>et al</i> , 1996 <sup>10</sup>
	<b>2</b>	<b>Glu22Lys</b>	<b>1 family</b>	<b>septal hypertrophy, benign course and prognosis</b>	<b>present study</b>
	3	Asn47Lys	1 individual	midventricular hypertrophy	Andersen <i>et al</i> , 2001 <sup>16</sup>
	4	<b>Arg58Gln</b>	2 families	septal hypertrophy, 2 sudden deaths	Flavigny <i>et al</i> , 1998 <sup>15</sup>
	<b>4</b>	<b>Arg58Gln</b>	<b>1 family</b>	<b>septal hypertrophy, malignant course/prognosis</b>	<b>present study</b>
	5	Pro94Arg	1 individual	no phenotype is described	Poetter <i>et al</i> , 1996 <sup>10</sup>
	5 and Intr. 6	Lys103Glu and IVS6-1*	1 family	septal hypertrophy, good prognosis and survival	Andersen <i>et al</i> , 2001 <sup>16</sup>
MYL3	3	Ala57Gly	2 families and 1 unrelated individual	septal hypertrophy, 2 sudden deaths	Lee W-H <i>et al</i> , 2001 <sup>59</sup>
	4	Met149Val	1 family	midventricular hypertrophy	Poetter <i>et al</i> , 1996 <sup>10</sup>
	4	Arg154His	1 individual	midventricular hypertrophy	Poetter <i>et al</i> , 1996 <sup>10</sup>

Note: the mutations identified in the present work are shown in bold; Intr. 6, intron 6; \*IVS6-1, a splice site mutation in intron 6.

This study presents two German families with the Glu22Lys and Arg58Gln mutations in the ventricular myosin regulatory light chain gene. The Glu22Lys and Arg58Gln variants have been previously observed in American and French HCM population, respectively.<sup>10,15</sup> The Glu22Lys mutation was identified in two brothers and one unrelated individual by Potter *et al*.<sup>10</sup>, whereas the Arg58Gln mutation was detected in two unrelated families by Flavigny *et al*.<sup>15</sup> In contrast to the previous study, this work presents a larger family spanning across three generations (family K) bearing the Glu22Lys mutation. However, the identified family with the Arg58Gln mutation (family B) was smaller than the two families described by Flavigny *et al*.<sup>15</sup> Two individuals in family B, who died suddenly, probably did had the Arg58Gln mutation, because, similarly to proband II-2, they suffered from HCM. Moreover, the proband and her deceased sister eventually inherited the Arg58Gln mutation from their deceased father, since their mother was genetically and clinically healthy.

That these two mutations cause HCM is supported by several observations. First, there was a clear cosegregation of the Glu22Lys and Arg58Gln mutation with HCM in the present and previous studies: the mutations were present in all clinically affected family members. Second, neither of these mutations was observed in control individuals (105 controls were screened in the present study) indicating that they are not common polymorphisms. Third, the altered residues as well as flanking sequences show strong evolutionary conservation across vertebrate species suggesting an important role for the RLC function (figure 3.7). Furthermore, the RLC carrying these mutations is a protein of the cardiac sarcomere: the causality of mutant sarcomeric proteins in HCM is well established.<sup>2,3</sup>

The identification of the Glu22Lys and Arg58Gln mutations in the different study populations suggests that the codons 22 and 58 are highly susceptible to mutations. Such hot spots have also been observed in the  $\beta$ -myosin heavy chain gene: mutations often affected codons encoding amino acids 403, 719 and 741.<sup>50</sup> Interestingly, different mutations were observed at these sites. Associated HCM phenotypes were generally different for distinct mutations but showed high similarity for the same mutations.<sup>50</sup> As discussed further, the HCM phenotypes observed in the present and previous studies were similar for the Arg58Gln but not for the Glu22Lys mutation.

### 4.3 Genotype-phenotype correlations

In the previous study by Potter *et al.*<sup>10</sup>, the Glu22Lys mutation was associated with a particular phenotype with massive hypertrophy of the cardiac papillary muscles and adjacent ventricular tissue causing midcavity obstruction, whereas the Arg58Gln mutation caused typical asymmetric septal hypertrophy in the study by Flavigny *et al.*<sup>15</sup> In the present study, the individuals bearing the Glu22Lys mutation had no massive midventricular hypertrophy with midcavity obstruction but asymmetric hypertrophy of interventricular septum. The individuals of family B with the Arg58Gln mutation also had asymmetric septal hypertrophy similar to that described by Flavigny *et al.*<sup>15</sup> These observations suggest that identical mutations in myosin light chains can cause diverse patterns of LV hypertrophy as mutations in other genes do. Furthermore, the midventricular hypertrophy was also observed in HCM cases caused by mutations in  $\beta$ -

myosin heavy chain and cardiac myosin binding protein C and is, therefore, not an unique feature of myosin light chain mutations.<sup>16,59</sup>

Concerning the disease course and prognosis, a recent study suggested that myosin light chain mutations cause only benign HCM phenotypes,<sup>16</sup> however, the present work shows that clinical course and prognosis associated with myosin regulatory light chain mutations can differ markedly. The Glu22Lys mutation was associated with a benign phenotype. Two affected individuals had reached an advanced age. There was no case of sudden cardiac death in the family, and most of the family members had only mild hypertrophy, a late onset of symptoms or no symptoms at all. In contrast, the Arg58Gln mutation identified in family B was associated with two cases of premature sudden cardiac death. Furthermore, myocardial hypertrophy developed in early childhood and was accompanied by disease symptoms as premature fatigue and later on as arrhythmias. Flavigny *et al.*<sup>15</sup> also reported two sudden deaths at young age in one of the identified families with the Arg58Gln mutation. Thus, pooled data from the study by Flavigny *et al.*<sup>15</sup> and the present work suggest that the Arg58Gln mutation indeed may cause a malignant HCM phenotype with a high risk of sudden death and, therefore, could be added to the panel of mutations associated with a poor prognosis (see table 1.1). Genotyping for such mutations could be recommended in order to improve risk stratification in HCM patients and early diagnosis of individuals in the need for prophylactic therapy. Apparently, the identification of more families with the Arg58Gln mutation will be of value in proving these observations.

The penetrance of HCM was demonstrated to vary widely.<sup>76</sup> Complete penetrance of familial HCM was shown to be a feature of some malignant mutations in  $\beta$ -myosin heavy chain.<sup>54</sup> Low disease penetrance is characteristic of mutations in cardiac troponin T<sup>77</sup> and myosin binding protein C.<sup>52</sup> Furthermore, the penetrance of cardiac myosin binding protein C mutations were shown to be age related: generally HCM develops after midlife.<sup>78</sup> Variable disease penetrance was also described for some previously identified RLC/ELC mutations.<sup>15,59</sup> Similarly, in family B and K the respective mutations penetrated to the HCM phenotypes differently. Although the Arg58Gln mutation was associated with complete disease penetrance, family B is too small to draw final conclusions. The Glu22Lys mutation, in contrast, showed reduced HCM penetrance (57%): among seven genetically affected individuals only four had apparent HCM. However, given the age-related penetrance of cardiac myosin binding

protein C mutations, it can be assumed that "healthy carriers" of family K may still develop HCM later on in their life and therefore need to be followed up.

It was also shown that not all HCM phenotypes, when expressed, manifest to the same degree, for instance, with regard to magnitude of LV hypertrophy and severity of clinical course.<sup>50,52</sup> Such variable expressivity is a typical feature of HCM and on certain extent, depends on the nature of the causative gene/mutation. Thus, malignant mutations in the  $\beta$ -myosin heavy chain gene, apart from complete penetrance, showed significant myocardial hypertrophy.<sup>54,79</sup> Cardiac troponin T gene mutations were generally associated with mild hypertrophy.<sup>53,77</sup> The extent of hypertrophy caused by mutations in the myosin light chain genes varied from mild to massive.<sup>10,15,59</sup> The Arg58Gln was associated with moderate hypertrophy in the previous and present studies, whereas the Glu22Lys mutation caused massive hypertrophy in the earlier study but not in this work.

The expressivity of HCM phenotypes was further shown to vary within the family members carrying exactly the same mutation.<sup>50,59</sup> This was also observed in family K and B. The proband of family B (II-2) had non-obstructive HCM, whereas her sister (II-1) exhibited obstruction of LV outflow tract with increased pressure gradient. In family K, the older individual showed moderate hypertrophy of the entire septum, while younger patients had mild mid- and basal septal hypertrophy.

Several mechanisms are implicated in the variability of the penetrance and expressivity in HCM.<sup>3</sup> The differences in the phenotypic expression and penetrance among causal genes could be explained by the functional role of the respective protein. Thus, in the case of  $\beta$ -myosin heavy chain mutations, more abundant phenotypes are expected considering the primary function of this protein in cardiac contraction. The diversity of phenotypes associated with mutations in the same disease gene may be due to the localization in differently important protein regions as well as to the kind of the mutation. Another contributing factor is the individual genetic background (*i.e.* modifier genes), which may have a modulatory role. Thus, in the case of family B and K, the distinct localization of the mutations within RLC may be responsible for the differences in phenotypic expression of HCM. Furthermore, the observed variable expressivity of mutations within the same families suggests the presence of specific modifier genes. Further studies of large numbers of families carrying the Glu22Lys and Arg58Gln mutations are necessary to clarify whether the observed malignant and

benign phenotypes are unique to these particular mutations and generally applicable, or whether they are due to the differences in genetic backgrounds in families B and K.

#### 4.4 Possible functional implications of the Glu22Lys and Arg58Gln mutations

The high evolutionary conservation of the amino acid residues affected by the Glu22Lys and Arg58Gln mutations suggests their essentiality for the RLC function. The full-length amino acid alignment (partly presented in figure 3.14) also showed that the highest sequence homology is shared by the RLCs from the same muscle type and, hence, with similar functions. This underlines that the amino acid sequence determines functional properties of the protein and, consequently, any alteration in this sequence will affect its function.

Possible functional implications of the Glu22Lys and Arg58Gln mutations have been studied by Szsesna *et al.*,<sup>29</sup> who investigated the effects of the Glu22Lys and Arg58Gln mutations on the RLC calcium-binding and phosphorylation properties. In that study, the Glu22Lys mutant could not be phosphorylated and had decreased  $\text{Ca}^{2+}$  affinity, whereas the Arg58Gln mutant did not bind  $\text{Ca}^{2+}$  at all.

In an earlier study, Levine *et al.*<sup>80</sup> investigated functional and structural consequences of the Glu22Lys mutation in deltoid muscle fibers obtained from a HCM patient carrying this mutation, since the same RLC isoform is expressed in both cardiac ventricle and slow twitch fibers of the deltoid muscle. The study revealed that the biopsied fibers show loss of the normal arrangement of myosin heads associated with the relaxed state. This eventually accounted for a local change in electrical charge caused by the Glu22Lys mutation; charge alteration subsequently may affect the normal RLC conformation and weaken the RLC structural support to the myosin neck. That the normal net charge of the RLC N-terminus is important for the RLC conformation and RLC-myosin interaction has been also shown in a study by Sweeney *et al.*<sup>81</sup>

Thus, the Glu22Lys and Arg58Gln mutations could alter the function of the molecular motor myosin by either eliminating the normal effects of RLC phosphorylation and calcium binding or by affecting the allosteric interaction of the myosin heavy

chain/RLC complex. This, consequently, may disturb the normal manner of the force generating myosin-actin interaction and lead to a contractile deficit. According to the current hypothesis on HCM pathogenesis, the impaired sarcomeric contractility induces increased expression of trophic factors in the heart, which leads to clinical and pathological phenotypes characteristic of HCM.<sup>24</sup> Further genetic and functional studies will hopefully help us to complete our understanding of the mechanisms that underlie the development of HCM, because the establishment of new efficient management strategies can be based only on accurate knowledge of both the etiologies and pathogenic mechanism of a disorder.

**In conclusion**, two mutations were identified in the ventricular myosin regulatory light chain gene and associated with either benign or malignant HCM phenotypes. The Glu22Lys mutation was associated with a late onset of clinical symptoms, benign course and good prognosis, whereas the Arg58Gln mutation was associated with an early onset of clinical manifestation and premature sudden cardiac death. These findings show that genotyping could give valuable information for the risk stratification, genetic counselling and treatment strategies in hypertrophic cardiomyopathy

## 5 References

1. Richardson P, McKenna W, Bristow M et al. Report of the 1995 World Health Organization/International Society and Federation of Cardiology Task Force on the Definition and Classification of cardiomyopathies. *Circulation* 1996; 93: 841-2.
2. Seidman JG, Seidman C. The genetic basis for cardiomyopathy: from mutation identification to mechanistic paradigms. *Cell* 2001; 104: 557-67.
3. Marian AJ and Robertrs R. The molecular genetic basis for cardiomyopathy. *J Mol Cell Cardiol* 2001; 33: 655-70.
4. Maron BJ, Gardin JM, Flack JM, Gidding SS, Kurosaki TT, Bild DE. Prevalence of hypertrophic cardiomyopathy in a general population of young adults. Echocardiographic analysis of 4111 subjects in the CARDIA Study. Coronary Artery Risk Development in (Young) Adults. *Circulation* 1995; 92: 785-9.
5. Maron BJ, Olivotto I, Spirito P et al. Epidemiology of hypertrophic cardiomyopathy-related death: revisited in a large non-referral-based patient population. *Circulation* 2000; 102: 858-64.
6. Teare RD. Asymmetrical hypertrophy of the heart in young adults. *Br Heart* 1958; 20: 1-8.
7. Geisterfer-Lowrance AA, Kass S, Tanigawa G et al. A molecular basis for familial hypertrophic cardiomyopathy: a beta cardiac myosin heavy chain gene missense mutation. *Cell* 1990; 62: 999-1006.
8. Thierfelder L, Watkins H, MacRae C et al. Alpha-tropomyosin and cardiac troponin T mutations cause familial hypertrophic cardiomyopathy: a disease of the sarcomere. *Cell* 1994; 77: 701-12.
9. Watkins H, Conner D, Thierfelder L et al. Mutations in the cardiac myosin binding



protein-C gene on chromosome 11 cause familial hypertrophic cardiomyopathy. *Nat Genet* 1995; 11: 434-7.

10. Poetter K, Jiang H, Hassanzadeh S et al. Mutations in either the essential or regulatory light chains of myosin are associated with a rare myopathy in human heart and skeletal muscle. *Nat Genet* 1996; 13: 63-9.

11. Kimura A, Harada H, Park JE et al. Mutations in the cardiac troponin I gene associated with hypertrophic cardiomyopathy. *Nat Genet* 1997; 16: 379-82.

12. Mogensen J, Klausen IC, Pedersen AK et al. Alpha-cardiac actin is a novel disease gene in familial hypertrophic cardiomyopathy. *J Clin Invest* 1999; 103: R39-43.

13. Satoh M, Takahashi M, Sakamoto T, Hiroe M, Marumo F, Kimura A. Structural analysis of the titin gene in hypertrophic cardiomyopathy: identification of a novel disease gene. *Biochem Biophys Res Commun* 1999; 262: 411-7.

14. Fung DC, Yu B, Littlejohn T, Trent RJ. An online locus-specific mutation database for familial hypertrophic cardiomyopathy. *Hum Mutat* 1999; 14: 326-32.

15. Flavigny J, Richard P, Isnard R et al. Identification of two novel mutations in the ventricular regulatory myosin light chain gene (MYL2) associated with familial and classical forms of hypertrophic cardiomyopathy. *J Mol Med* 1998; 76: 208-14.

16. Andersen PS, Havndrup O, Bundgaard H et al. Myosin light chain mutations in familial hypertrophic cardiomyopathy: phenotypic presentation and frequency in Danish and South African populations. *J Med Genet* 2001; 38: E43.

17. Dalloz F, Osinska H, Robbins J. Manipulating the contractile apparatus: genetically defined animal models of cardiovascular disease. *J Mol Cell Cardiol* 2001; 33: 9-25.

18. Marian AJ, Wu Y, Lim DS et al. A transgenic rabbit model for human hypertrophic cardiomyopathy. *J Clin Invest* 1999; 104: 1683-92.

19. Seiler SH, Fischman DA, Leinwand LA. Modulation of myosin filament organization by C-protein family members. *Mol Biol Cell* 1996; 7: 113-27.

20. *Harrison's principles of internal Medicine*. 14th edition. Fauci AS, Braunwald E, Isselbacher KJ et al. USA 1998; chapter 232: p1279.

21. Rayment I, Rypniewski WR, Schmidt-Base K et al. Three-dimensional structure of myosin subfragment-1: a molecular motor. *Science* 1993; 261: 50-8.

22. Mulvihill DP and Hyams JS. Shedding a little light on light chains. *Nature Cell Biology* 2001; 3:E1-2.
23. Alberts B, Bray D, Lewis J, Raff M, Roberts K, Watson JD. *Molecular biology of the cell*. 3rd ed. USA 1994; chapter 16: pp 847-858.
24. Marian AJ. Pathogenesis of diverse clinical and pathological phenotypes in hypertrophic cardiomyopathy. *Lancet* 2000; 355: 58-60.
25. Macera MJ, Szabo P, Wadgaonkar R, Siddiqui MA, Verma RS. Localization of the gene coding for ventricular myosin regulatory light chain (MYL2) to human chromosome 12q23-q24.3. *Genomics* 1992; 13: 829-31.
26. Fodor WL, Darras B, Seharaseyon J, Falkenthal S, Francke U, Vanin EF. Human ventricular/slow twitch myosin alkali light chain gene characterization, sequence, and chromosomal location. *Nature* 1985; 315: 37-40.
27. Babu YS, Sack JS, Greenhough, Bugg cE, Means AR, Cook WJ. Three-dimensional structure of calmodulin. *J Biol Chem* 1989; 264: 2143-9.
28. daSilva AC, Reinach FC. Calcium binding induces conformational changes in muscle regulatory proteins. *Trends Biochem Sci* 1991; 16: 53-7.
29. Szczesna D, Ghosh D, Li Q et al. Familial hypertrophic cardiomyopathy mutations in the regulatory light chains of myosin affect their structure, Ca<sup>2+</sup> binding, and phosphorylation. *J Biol Chem* 2001; 276: 7086-92.
30. Morano I. Tuning the human heart molecular motors by myosin light chains. *J Mol Med* 1999; 77: 544-55.
31. Uyeda TQ, Abramson PD, Spudich JA. The neck region of the myosin motor domain acts as a lever arm to generate movement. *Proc Natl Acad Sci U S A* 1996; 93: 4459-64.
32. Lowey S, Waller GS, Trybus KM. Skeletal muscle myosin light chains are essential for physiological speeds of shortening. *Nature* 1993; 365: 454-6.
33. Lowey S, Trybus KM. Role of skeletal and smooth muscle myosin light chains. *Biophys J* 1995; 68: 120S-127S.
34. Trybus KM. Role of myosin light chains. *J Muscle Res Cell Motil* 1994; 15: 587-94.

35. Sweeney HL, Stull JT. Alteration of cross-bridge kinetics by myosin light chain phosphorylation in rabbit skeletal muscle: implications for regulation of actin-myosin interaction. *Proc Natl Acad Sci U S A* 1990; 87: 414-8.
36. Sweeney HL, Bowman BF, Stull JT. Myosin light chain phosphorylation in vertebrate striated muscle: regulation and function. *Am J Physiol* 1993; 264: C1085-95.
37. Levine RJ, Kensler RW, Yang Z, Sweeney HL. Myosin regulatory light chain phosphorylation and the production of functionally significant changes in myosin head arrangement on striated muscle thick filaments. *Biophys J* 1995; 68: 224S.
38. Levine RJ, Kensler RW, Yang Z, Stull JT, Sweeney HL. Myosin light chain phosphorylation affects the structure of rabbit skeletal muscle thick filaments. *Biophys J* 1996; 71: 898-907.
39. Szczesna D, Zhao J, Guzman G, Zhi G, Stull D, Potter JD. Phosphorylation and Ca<sup>2+</sup> binding to the regulatory light chains of myosin in the regulation of skeletal muscle contraction. *Biophys J* 1997; 72: A175.
40. Roberts R, Sigwart U. New concepts in hypertrophic cardiomyopathies, part II. *Circulation* 2001; 104: 2249-52.
41. Wigle ED. Cardiomyopathy: The diagnosis of hypertrophic cardiomyopathy. *Heart* 2001; 86: 709-14.
42. *Heart Disease. A textbook of cardiovascular Medicine*. 5th edition. Braunwald E. USA 1997; chapter 41: p 1421.
43. McKenna WJ, Spirito P, Desnos M, Dubourg O, Komajda M. Experience from clinical genetics in hypertrophic cardiomyopathy: proposal for new diagnostic criteria in adult members of affected families. *Heart* 1997; 77: 130-2.
44. Spirito P, Bellone P, Harris KM, Bernabo P, Bruzzi P, Maron BJ. Magnitude of left ventricular hypertrophy and risk of sudden death in hypertrophic cardiomyopathy. *N Engl J Med* 2000; 342: 1778-85.
45. Maron BJ, Gottdiener JS, Epstein SE. Patterns and significance of distribution of left ventricular hypertrophy in hypertrophic cardiomyopathy. A wide angle, two dimensional echocardiographic study of 125 patients. *Am J Cardiol* 1981; 48: 418-28.
46. Elliott PM, Poloniecki J, Dickie S et al. Sudden death in hypertrophic cardiomyopathy: identification of high risk patients. *J Am Coll Cardiol* 2000; 36: 2212-8.

47. Maron BJ. Ventricular arrhythmias, sudden death, and prevention in patients with hypertrophic cardiomyopathy. *Curr Cardiol Rep* 2000; 2: 522-8.
48. Fatkin D, Graham RM. Prognostic value of left ventricular hypertrophy in hypertrophic cardiomyopathy. *N Engl J Med* 2001; 344: 63-5.
49. Elliott PM, Gimeno Blanes JR, Mahon NG, Poloniecki JD, McKenna WJ. Relation between severity of left-ventricular hypertrophy and prognosis in patients with hypertrophic cardiomyopathy. *Lancet* 2001; 357: 420-4.
50. Tesson F, Richard P, Charron P et al. Genotype-phenotype analysis in four families with mutations in beta-myosin heavy chain gene responsible for familial hypertrophic cardiomyopathy. *Hum Mutat* 1998; 12: 385-92.
51. Charron P, Dubourg O, Desnos M et al. Genotype-phenotype correlations in familial hypertrophic cardiomyopathy. A comparison between mutations in the cardiac protein-C and the beta-myosin heavy chain genes. *Eur Heart J* 1998; 19: 139-45.
52. Charron P, Dubourg O, Desnos M et al. Clinical features and prognostic implications of familial hypertrophic cardiomyopathy related to the cardiac myosin-binding protein C gene. *Circulation* 1998; 97: 2230-6.
53. Watkins H, McKenna WJ, Thierfelder L et al. Mutations in the genes for cardiac troponin T and alpha-tropomyosin in hypertrophic cardiomyopathy. *N Engl J Med* 1995; 332: 1058-64.
54. Hwang TH, Lee WH, Kimura A et al. Early expression of a malignant phenotype of familial hypertrophic cardiomyopathy associated with a Gly716Arg myosin heavy chain mutation in a Korean family. *Am J Cardiol* 1998; 82: 1509-13.
55. Erdmann J, Raible J, Maki-Abadi J et al. Spectrum of clinical phenotypes and gene variants in cardiac myosin-binding protein C mutation carriers with hypertrophic cardiomyopathy. *J Am Coll Cardiol* 2001; 38: 322-30.
56. Maron BJ. Hypertrophic cardiomyopathy. *Lancet* 1997; 350: 127-33.
57. Ortlepp JR, Vosberg HP, Reith S et al. Genetic polymorphisms in the rennin-angiotensin-aldosterone system associated with expression of left ventricular hypertrophy in hypertrophic cardiomyopathy: a study of five polymorphic genes in a family with a disease causing mutation in the myosin binding protein C gene. *Heart* 2002; 87: 270-275.

- 
58. Roberts R, Sigwart U. New concepts in hypertrophic cardiomyopathies, part I. *Circulation* 2001; 104: 2113-16.
59. Lee WH, Hwang TH, Kimura A et al. Different expressivity of a ventricular essential myosin light chain gene Ala57Gly mutation in familial hypertrophic cardiomyopathy. *Am Heart J* 2001; 141: 184-9.
60. Henry WL, DeMaria A, Gramiak R et al. Report of the american society of echocardiography committee on nomenclature and standards in two-dimensional echocardiography. *Circulation* 1980; 62: 212-5.
61. Henry WL, Gardin JM, Ware JH. Echocardiographic measurements in normal subjects from infancy to old age. *Circulation* 1980; 62: 1054-61.
62. Lahiri DK, Nurnberger JI. A rapid non-enzymatic method for the preparation of HMW DNA from blood for RFLP studies. *Nucleic Acids Res* 1991; 19: 5444.
63. Hayashi K, Yandell DW. How sensitive is PCR-SSCP? *Hum Mutat* 1993; 2: 338-46.
64. Condie A, Eeles R, Borresen AL, Coles C, Cooper C, Prosser J. Detection of point mutations in the p53 gene: comparison of single-strand conformation polymorphism, constant denaturant gel electrophoresis, and hydroxylamine and osmium tetroxide techniques. *Hum Mutat* 1993; 2: 58-66.
65. Dunnen JT and Antonarakis SE. Mutation nomenclature extensions and suggestions to describe complex mutations. *Hum Mutat* 2000; 15: 7-12.
66. Miura K, Nakagawa H, Morikawa et al. Epidemiology of idiopathic cardiomyopathy in Japan: results from nationwide survey. *Heart* 2002; 87: 126-30.
67. Grompe M. The rapid detection of unknown mutations in nucleic acids. *Nat Genet* 1993; 5: 111-7.
68. Orita M, Suzuki Y, Sekiya T, Hayashi K. Rapid and sensitive detection of point mutations and DNA polymorphisms using the polymerase chain reaction. *Genomics* 1989; 5: 874-9.
69. Glavac D, Dean M. Optimization of the single-strand conformation polymorphism (SSCP) technique for detection of point mutations. *Hum Mutat* 1993; 2: 404-14.
70. Lewis R. SNPs as windows on evolution. *The Scientist* 2002; 16: 16-18.

71. Syvanen AC, Landegren U, Isaksson A, Gyllensten U, Brookes A. First International SNP Meeting at Skokloster, Sweden, August 1998. Enthusiasm mixed with scepticism about single-nucleotide polymorphism markers for dissecting complex disorders. *Eur J Hum Genet* 1999; 7: 98-101.
72. Sachidanandam R, Weissman D, Schmidt SC et al. A map of human genome sequence variation containing 1.42 million single nucleotide polymorphisms. *Nature* 2001; 409: 928-33.
73. Geraghty DE, Vu Q, Williams L et al. Mapping HLA for single nucleotide polymorphisms. *Rev Immunogenet* 1999; 1: 231-8.
74. Martin ER, Lai EH, Gilbert JR et al. SNPping away at complex diseases: analysis of single-nucleotide polymorphisms around APOE in Alzheimer disease. *Am J Hum Genet* 2000; 67: 383-94.
75. Herrmann S, Schmidt-Petersen K, Pfeifer J et al. A polymorphism in the endothelin-A receptor gene predicts survival in patients with idiopathic dilated cardiomyopathy. *Eur Heart J* 2001; 22: 1948-53.
76. Charron P, Carrier L, Dubourg O et al. Penetrance of familial hypertrophic cardiomyopathy. *Genet Couns* 1997; 8: 107-14.
77. Moolman JC, Corfield VA, Posen B et al. Sudden death due to troponin T mutations. *J Am Coll Cardiol* 1997; 29: 549-55.
78. Maron BJ, Niimura H, Casey SA et al. Development of left ventricular hypertrophy in adults in hypertrophic cardiomyopathy caused by cardiac myosin-binding protein C gene mutations. *J Am Coll Cardiol* 2001; 38: 315-21.
79. Ko YL, Chen JJ, Tang TK et al. Malignant familial hypertrophic cardiomyopathy in a family with a 453Arg-Cys mutation in the  $\beta$ -myosin heavy chain gene: coexistence of sudden death and end-stage heart failure. *Hum Gen* 1996; 97: 585-90.
80. Levine RJ, Yang Z, Epstein ND, Fananapazir L, Stull JT, Sweeney HL. Structural and functional responses of mammalian thick filaments to alterations in myosin regulatory light chains. *J Struct Biol* 1998; 122: 149-61.
81. Sweeney HL, Yang Z, Zhi G, Stull JT, Trybus KM. Charge replacement near the phosphorylatable serine of the myosin regulatory light chain mimics aspects of phosphorylation. *Proc Natl Acad Sci Usa* 1994; 91: 1490-94.

## List of abbreviations

A	adenine
APS	ammonium persulphate
Arg	arginine
ATP	adenosine triphosphate
Asn	asparagine
Asp	aspartic acid
bp	base pair
BSA	body surface area
10xBSA	10xbovine serum albumine
C	cytosine
Ca <sup>2+</sup>	calcium ion
cDNA	complementary DNA
Cys	cysteine
del	deletion
dATP	2'-deoxyadenosine-5'-triphosphate
dCTP	2'-deoxycytidine-5'-triphosphate
dGTP	2'-deoxyguanosine-5'-triphosphate
dTTP	2'-deoxythymidine-5'-triphosphate
ddATP	2',3'-dideoxyadenosine-5'-triphosphate
ddCTP	2',3'-dideoxycytidine-5'-triphosphate
ddGTP	2',3'-dideoxyguanosine-5'-triphosphate
ddNTP	2',3'-dideoxynucleoside-5'-triphosphate
ddTTP	2',3'-dideoxthymidine-5'-triphosphate
DNA	deoxyribonucleic acid
dNTP	2'-deoxynucleotide-5'-triphosphate
7-deaza-dGTP	7-deaza-2'-deoxyguanosine-5'triphosphate
E	glutamic acid

ECG	electrocardiography
EDTA	ethylenediaminetetraacetic acid
EF-hand domain	calcium ion binding domain
ELC	essential light chain
FAM	5-carboxy-fluorescein
G	guanine
Gln	glutamine
Glu	glutamic acid
Gly	glycine
g	gram
h	hour
HCl	hydrochloric acid
HCM	hypertrophic cardiomyopathy
His	histidine
ICD	implantable cardioverter defibrillator
Ile	isoleucine
ins	insertion
IVS	interventricular septum
JOE	2', 7'-dimethoxy-4', 5'-dichloro-6-fluorescein
K	lysine
KCl	potassium chloride
Leu	leucine
Lys	lysine
LV	left ventricle
LVEED	left ventricle end-diastolic dimension
LVOT	left ventricular outflow tract



M	molar (mol/l)
Maron type	type of left ventricular hypertrophy distribution
Met	methionine
MDE-solution	mutation detection enhancement solution
MDE-F	MDE solution with formamide
mg	milligram
min	minute
ml	milliliter
mM	millimolar
MLC-1s/v	myosin light chain 1 slow/ventricular
MLC-2s/v	myosin light chain 2 slow/ventricular
mmol	milimol
<i>MYL2</i>	ventricular myosin regulatory light chain gene
<i>MYL3</i>	ventricular myosin essential light chain gene
μl	microliter
NaCl	sodium chloride
ng	nanogram
nm	nanometer
N-terminal	amino terminal
10xNEBuffer	New England Biolabs buffer
NYHA class	New York Heart Association class of heart failure
6% PAA	6% polyacrylamide gel solution
PCR	polymerase chain reaction
pH	negative log of hydrogen ion concentration
Phe	phenylalanine
PW	posterior wall
Pro	proline
Q	glutamine
R	arginine

Ref	reference
RFLP	restriction fragment length polymorphism
RLC	regulatory light chain
ROX	6-carboxy-X-rhodamin
rpm	revolutions per minute
SAM	systolic anterior motion of mitral valve
SCD	sudden cardiac death
sec	second
Ser	serine
SDS	sodium dodecyl sulfate
SNP	single nucleotide polymorphism
<i>Sty</i> I	restriction enzyme
SSCP	single strand conformation polymorphism
T	thymine
TAMRA	N, N, N', N'-tetramethyl-6-carboxyrhodamin
<i>Taq</i> <sup>α</sup> I	restriction enzyme
TBE	Tris-Boric acid-EDTA buffer
TEMED	N, N, N', N'-tetramethyl-ethylendiamine
Tris	tris (hydroxymethyl)-aminomethane
Trp	tryptophan
Tyr	tyrosine
Val	valine

## Appendix

### A. Acknowledgements

I sincerely thank all my colleagues and friends in Berlin and Bishkek for their help and support during this project.

I am very much grateful to Prof. Dr. med. K. J. Osterziel for giving me an opportunity to carry out this work. I also wish to express my gratitude to Prof. M. M. Mirrakhimov for his constant support and encouragement. My special thanks goes to my supervisor Andreas Perrot, who put a lot of effort and time in guiding my project. I also thank him for his valuable comments on this manuscript. I am very much thankful to Mrs. U. Weiher for her everyday help and to Sabine Haßfeld for usefull discussions and advices on this manuscript. I would like to acknowledge Dr. N. Bit-Avragim for her help in the beginning of my work and Petra Schirmacher for her technical assistance.

My warm thanks go to Dr. Swaroop Bhojani, Kamal Sharma, Hari Easwaran and Dheeraj Khare, whose assistance, friendship and constant encouragement, supported me throughout this work. I also thank Dheeraj, Hari and Kamal for their comments on this manuscript.

Finally, I thank my family members for their patience, support and love.

## B. Curriculum Vitae

Name: Zhyldyz Temirzhanovna Kabaeva  
 Date and place of birth: 21.10.1972, Djany-Alysh (Kyrgyzstan)  
 Marital status: single  
 Nationality: Kyrgyz

### Education

09.1979 – 06.1989 Certificate of Secondary School Education.  
 Secondary School #7. Tokmok. Kyrgyzstan.

08.1989 – 06.1995 Medical Diploma of General Practitioner in Medicine.  
 Kyrgyz State Medical Institute. Bishkek. Kyrgyzstan

09.1995 – 07.1997 Post-graduate clinical training course in Internal Medicine and  
 Cardiology.  
 National Centre of Cardiology and Internal Medicine. Bishkek.  
 Kyrgyzstan.

10.1999 – 2002 MD-PhD student Thesis title: Genetic analysis in hypertrophic  
 cardiomyopathy: missense mutations in the ventricular myosin  
 regulatory light chain gene.  
 Charité/Franz-Volhard-Klinik at Max-Delbrück-Centrum für molekulare  
 Medizin Humboldt-Universität zu Berlin. Berlin. Germany.  
 Supervisors: Prof. Dr. med. K. J. Osterziel and Dipl.-Ing. A. Perrot

### Work experience

09.1997 – 03.1999 Medical Doctor at Cardiology Intensive Care Department  
 National Centre of Cardiology and Internal Medicine.  
 Bishkek. Kyrgyzstan.

### Research experience

09.1997 – 06.1999 Research duties at Department of non-invasive diagnostic methods:  
 Clinical and Echo evaluation of patients with cardiomyopathies  
 National Centre of Cardiology and Internal Medicine. Bishkek.  
 Kyrgyzstan

10.1999 – 2002 Molecular genetics of cardiomyopathies: identification of causative  
 genes and mutations in patients with Hypertrophic and Dilated  
 Cardiomyopathies using PCR, single strand conformation polymorphism  
 analysis, restriction fragment length polymorphism analysis, and direct  
 automated DNA sequencing. Genotype-phenotype correlations.  
 CardioGenetic Laboratory. Charité/Franz-Volhard-Klinik. Berlin.  
 Germany

### Awards and honours

06.1999 – 07.2000 Awarded the DAAD fellowship for research in molecular aspects of  
 Familial Cardiomyopathies in Germany.

**Publications**

**Zhyldyz T Kabaeva**, Andreas Perrot, Bastian Wolter, Rainer Dietz, Nuno Cardim, João Martins Correia, Hagen D. Schulte, Almaz A. Aldashev, Mirsaid M. Mirrakhimov, Karl Josef Osterziel. "Systematic analysis of the regulatory and essential light chain genes: genetic variants and mutations in hypertrophic cardiomyopathy". European Journal of Human Genetics 2002; 10:741-748.

N. Bit-Avragim, A. Perrot, **Z. Kabaeva**, D. Usupbaeva, R. Rudenko, B. Imanov, B. Isalieva, H. Schmidt-Traub, B. Hoffmann, M.M. Mirrakhimov, R. Geßner, K.J. Osterziel. "Novel mutations in the  $\beta$ -myosin heavy chain gene in Kyrgyz families with hypertrophic cardiomyopathy". 66. Jahrestagung der Deutschen Gesellschaft für Kardiologie-Herz- und Kreislaufforschung, April 2000, Mannheim.

A. Perrot, **Z. Kabaeva**, C. Geier, N. Bit-Avragim, R. Bergmann-Lips, E. von Hodenberg, P. Binner, T. Scheffold, K.J. Osterziel. "Die Mutation Arg58Gln für die Regulatorische Myosin Leichtkette ist assoziiert mit plötzlichen Herztod". 67. Jahrestagung der Deutschen Gesellschaft für Kardiologie-Herz- und Kreislaufforschung, April 2001, Mannheim.

**Z. Kabaeva**, A. Perrot, C. Geier, M. Fitschen, N. Bit-Avragim, P. Binner, T. Scheffold, N Cardim, K.J. Osterziel. "The mutation Arg58Gln in the regulatory myosin light chain gene is associated with sudden cardiac death". XXII Annual Congress of the European Society of Cardiology, September 2001, Stockholm.

### **C. Statement / Erklärung an Eides Statt**

I hereby declare that the present manuscript is my own work without use of any outside help. This manuscript contains no parts of other work.

Hiermit versichere ich, dass ich die vorliegende Arbeit selbständig verfasst und keine anderen als die angegebenen Hilfsmittel und Quellen benutzt habe. Die Arbeit darstellt auch in Teilen keine Kopie andere Arbeiten.

Zhyldyz Kabaeva

Berlin

07.05.2002